R-08-108

SR-Site Pre-modelling: Sensitivity studies of hydrogeological model variants for the Laxemar site using CONNECTFLOW

Steven Joyce, Jaap Hoek, Lee Hartley
Serco

Niko Marsic
Kemakta Konsult AB

December 2010

Svensk Kärnbränslehantering AB
Swedish Nuclear Fuel
and Waste Management Co

Box 250, SE-101 24 Stockholm
Phone +46 8 459 84 00

ISSN 1402-3091
SKB R-08-108

SR-Site Pre-modelling: Sensitivity studies of hydrogeological model variants for the Laxemar site using CONNECTFLOW

Steven Joyce, Jaap Hoek, Lee Hartley
Serco

Niko Marsic
Kemakta Konsult AB

December 2010

Keywords: Hydrogeology, Modelling, Laxemar

Abstract

This study investigated a number of potential model variants of the SR-Can hydrogeological models of the temperate period and the sensitivity of the performance measures to the chosen parameters. This will help to guide the choice of potential variants for the SR-Site project and provide an input to design premises for the underground construction of the repository.

It was found that variation of tunnel backfill properties in the tunnels had a significant effect on performance measures, but in the central area, ramps and shafts it had a lesser effect for those property values chosen. Variation of tunnel EDZ properties only had minor effects on performance measures.

The presence of a crown space in the deposition tunnels had a significant effect on the tunnel performance measures and a lesser effect on the rock and EDZ performance measures.

The presence of a deposition hole EDZ and spalling also had an effect on the performance measures.

Sammanfattning

Föreliggande studie har undersökt ett antal potentiella modellvarianter av den hydrogeologiska modellen i SR-Can för den tempererade perioden. Känsligheten i olika prestandamått för de valda parametrarna har undersökts. Detta underlättar valet av potentiella varianter för SR-Site projektet och ger input till konstruktionsförutsättningarna av förvaret.

Resultaten visar att en ändring av tunnelåterfyllningsegenskaperna har en signifikant påverkan på prestandamåtten, men i centralområdet, ramp och schakt har återfyllningsegenskaperna en mindre påverkan på prestandamåtten. Ändring av EDZ-egenskaperna i tunnlarna har enbart en mindre påverkan på prestandamåtten.

Förekomsten av en så kallad Crown space (konsolidering av återfyllningsmaterialet under tunnel-taket) i deponeringstunnlarna har en signifikant påverkan på tunnelns prestandamått, men en mindre påverkan på prestandamåtten för berg och EDZ.

Förekomsten av en EDZ och spjälkning i deponeringshålen har också en påverkan på prestandamåtten.

Contents

1 Introduction

1.1 Background

This project concerns modelling of the groundwater pathways from the repository for a release scenario during the temperate climate period. As part of the SR-Site modelling project it will be necessary to investigate a number of variants as a means to identify which model components and parameters will have an impact on site performance. This study investigated a number of potential variants of the SR-Can models and the sensitivity of the performance measures to the chosen parameters. This will help to suggest which variants will be important for the SR-Site project. The results of this study may also provide an input to design premises for the underground construction of the repository.

1.2 Scope and objectives

This project aims to investigate the sensitivity of site performance measures to a number of model variants. These variants are split into three groups as follows:

1. Variation of tunnel backfill properties.
2. Adding tunnel crown space and variation of EDZ properties.
3. Adding deposition hole EDZ and spalling.

The study is restricted to variations around the Laxemar base case in SR-Can, which may limit the generality of the results with respect to sites with very different distributions of water conducting fractures.

1.3 This report

This report describes a base case model that is derived from the original SR-Can base case model and gives the performance measures calculated for that case along with associated plots. The following sections each describe a variant model and the performance measures calculated in each case. A summary of the cases is provided in Table 1-1. For each variant, a comparison of the results is made to the base case or other variants as appropriate. Plots for the variant results are given when they illustrate a difference to the base case results.

Finally a summary is given that highlights the most significant findings of the report.

Table 1-1. Summary of cases.

Case	Section	Description
Base	2.2	The SR-Can base case, but with an EDZ transmissivity of 10^{-8} m^2/s and thickness of 0.3 m.
Degraded backfill	2.3	Hydraulic conductivity of the main, transport and deposition tunnels increased from 10^{-10} m/s to 10^{-8} m/s.
Enhanced central area, ramps and shafts	2.4	Hydraulic conductivity of the central area, ramp and shaft backfill reduced from 10^{-5} m/s to 10^{-8} m/s.
Crown space	3.1	Crown space added with a hydraulic conductivity of 10^{-3} m/s and a thickness of 0.1 m.
Crown space, degraded backfill	3.2	Crown space added and hydraulic conductivity of the deposition tunnels increased from 10^{-10} m/s to 10^{-8} m/s.
Crown space, less transmissive tunnel EDZ	3.3	Crown space added and transmissivity of the deposition tunnel EDZ reduced from 10^{-8} m^2/s to 10^{-10} m^2/s.
Deposition hole EDZ	4.1	EDZ added to deposition holes with a transmissivity of 10^{-9} m^2/s and a thickness of 0.1 m.
Deposition hole EDZ and spalling	4.2	EDZ and spalling added to deposition holes, the latter with a transmissivity of 10^{-5} m^2/s and a thickness of 0.1 m.
Deposition hole EDZ and spalling, degraded deposition tunnel EDZ	4.3	EDZ and spalling added to deposition holes, with the transmissivity of the deposition tunnel EDZ increased from 10^{-8} m^2/s to 10^{-6} m^2/s

2 Sensitivity analysis of tunnel backfill

2.1 Background

An indication of how sensitive the groundwater pathways are to tunnel backfill properties is required. The ConnectFlow models developed for SR-Can for Laxemar will be used as a basis for quantifying sensitivities. In SR-Can, the tunnel backfill hydraulic conductivity was set to 10^{-10} m/s in the base case and 10^{-8} m/s in a degraded backfill variant. In SR-Can, the EDZ properties were based on an appropriate geometric mean for the rock, enhanced by some factor. Both here and in SR-Can, sensitivities are quantified in terms of comparing groundwater performance measures (travel-time, initial Darcy flux, path length and flow-related transport resistance) for rock, tunnel and EDZ for each release point (fracture, EDZ and tunnel).

The base case for this task is a backfill hydraulic conductivity of 10^{-10} m/s in the tunnels at repository depth, but 10^{-5} m/s (representing gravel) in the central area, the ramp and shafts. For the EDZ, the design premise is that the transmissivity will be 10^{-8} m^2/s over a thickness of 0.3 m. Therefore, an updated base case needs to first be made with these new properties as a proper reference for sensitivity cases, and so that the relative importance of tunnel and EDZ paths can be assessed. The EDZ properties will then be held fixed for the tunnel sensitivity cases.

As well as the engineered components evolving in time, the natural system is also evolving due to processes such as land-rise and climate evolution. In SR-Can, flow conditions were considered from 2020 AD up to 10,000–20,000 years into the future. It was decided that the flow conditions at 2020 AD will suffice as a demonstration of sensitivities.

2.2 Laxemar base case

Model description

The base case model is taken from the SR-Can modelling study for Laxemar, as described fully in /Hartley et al. 2006/. Because of the computational size of the DFN models, two different scales of DFN model are required. The first is a detailed repository-scale model that models the repository explicitly as a CPM surrounded by a DFN model, as illustrated in Figure 2-1, with fractures down to a scale of order 1 m radius to resolve the release of particles from a canister and then advect them through the surrounding rock. However, this type of model has a limited domain, so it cannot necessarily model transport to the ground surface for all flow-paths, particularly long horizontal paths. Hence, a second type of nested model is constructed where a local-scale DFN model is embedded within a regional-scale ECPM model, as illustrated in Figure 2-2. The repository is modelled as equivalent fractures with appropriate properties. In this case, it is only possible to include fractures down to a radius of 8 m. This approach allows flow-paths to be continued from the repository-scale to the regional-scale within a consistent DFN representation to maintain realism in the calculation of performance measures such as the flow-related transport resistance.

The properties used for repository features in the base case model are given in Table 2-1. Other model properties are as described in /Hartley et al. 2006/. Note that the EDZ is only present below the deposition tunnels.

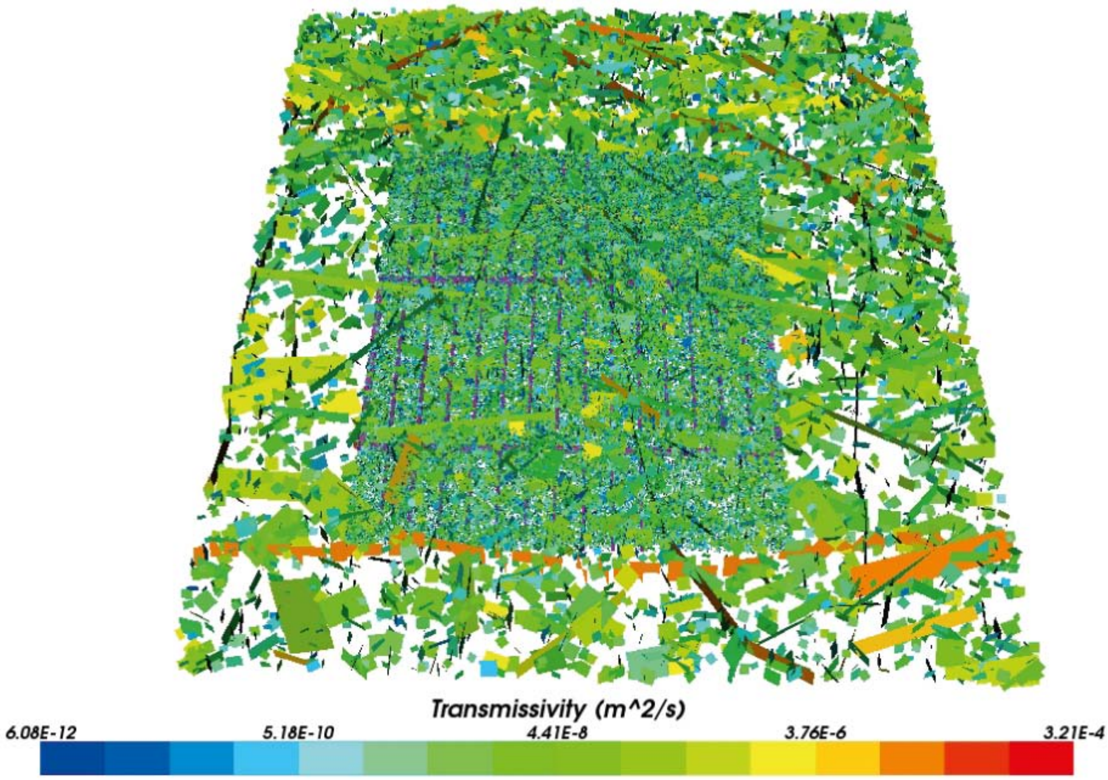

Figure 2-1. *An example of a combined DFN/CPM CONNECTFLOW model using a CPM sub-model of deposition and access tunnels nested within a DFN sub-model. Some fractures have been removed to reveal the tunnels. Here, the interface between the two sub-models is on the boundary of the CPM model.*

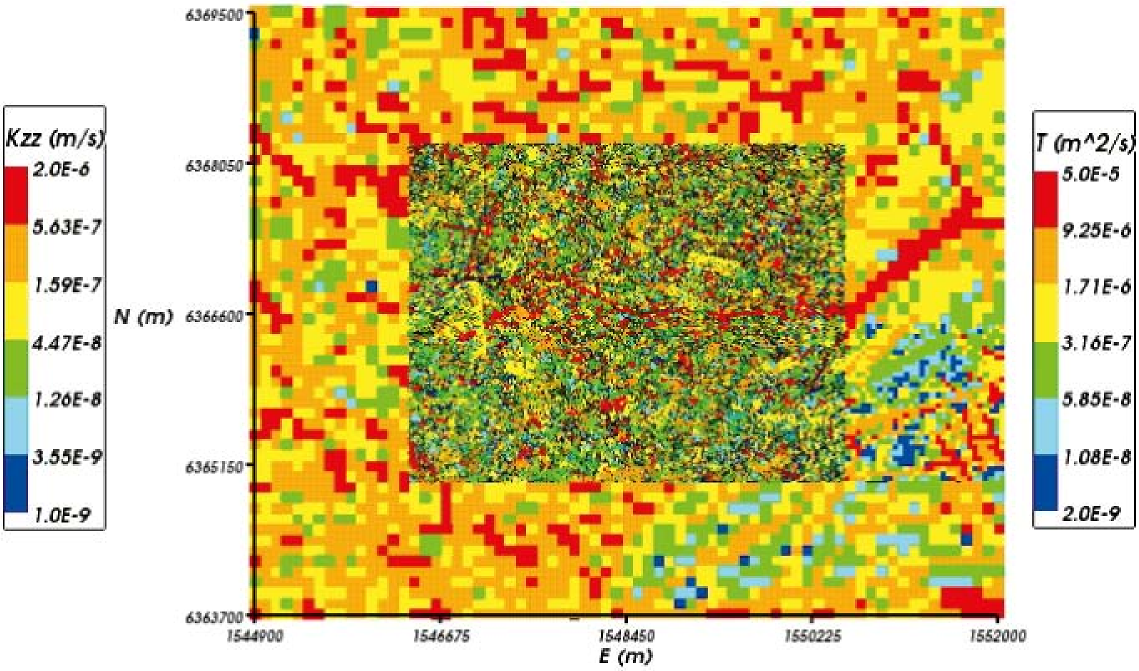

Figure 2-2. *An example of a combined ECPM/DFN CONNECTFLOW model using a DFN sub-model in the centre to represent the detailed fractures around a repository and nested within a larger regional-scale ECPM sub-model. In this map view fractures are coloured by transmissivity while ECPM elements are coloured by vertical hydraulic conductivity. Here, the interface between the two sub-models is on the boundary of the DFN model.*

Table 2-1. Base case properties for repository features.

Parameter	Value
Main tunnel hydraulic conductivity	10^{-10} m/s
Transport tunnel hydraulic conductivity	10^{-10} m/s
Deposition tunnel hydraulic conductivity	10^{-10} m/s
Central area hydraulic conductivity	10^{-5} m/s
Ramp and shaft hydraulic conductivity	10^{-5} m/s
Deposition hole hydraulic conductivity	10^{-11} m/s
Deposition tunnel EDZ transmissivity	10^{-8} m^2/s
Tunnel, central area, ramp and shaft backfill porosity	0.35
Deposition tunnel EDZ porosity	10^{-4}
Deposition tunnel EDZ thickness	0.3 m

Particle release points

As described in /Hartley et al. 2006/, three particles, corresponding to three path types, are released around each canister:

1. Q1 in the fracture with the highest flux that intersects the deposition hole;
2. Q2 in the tunnel EDZ fracture adjacent to the deposition hole;
3. Q3 in the CPM tunnel 1 m directly above the deposition hole.

A total of 22,449 (3 x 7,483) particles are released, three for each deposition hole. Particles are first tracked until they reach the boundary of the repository-scale model. This approach allows particles to move from the DFN sub-model to the CPM sub-model, or vice versa, any number of times according to the flow-field and so particles may pass through one or more sections of tunnel. To compute a complete path from a canister to the surface, once the particle exits the repository-scale model, the particle is restarted in the regional-scale DFN flow-field corresponding to the same release time.

Figure 2-3 shows the release points in the repository in blue and the exit locations at the regional model boundary in red.

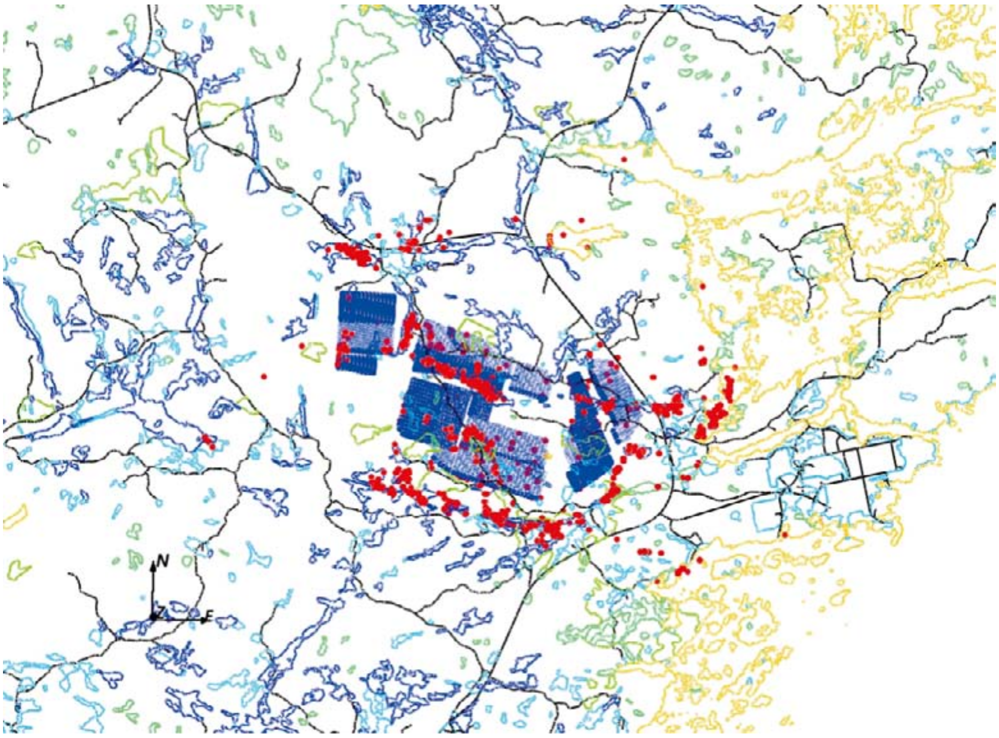

Figure 2-3. *Particle release and exit points viewed from above, for paths Q1, Q2 and Q3 in the base case of the amalgamated repository-scale and regional-scale DFN models with 7,483 particles released at time 2020 AD. Release points are coloured blue and exit locations are coloured red.*

Performance measures

The travel time (*t*), path length (*L*), initial Darcy flux (*U*) and flow-related transport resistance (*F*) performance measures are calculated from the particle tracking output as described in /Hartley et al. 2006/. These are sub-divided into values for the tunnels (t), the EDZ and the rock (r). The performance measures are accumulated in the rock, tunnels and EDZ separately as the particles move in and out of these sections. So for instance, L_r, gives the path length in the rock only and does not include the path length accumulated in the tunnels and EDZ. A summary of the performance measures reported here is given in Table 2-2.

Table 2-2. Summary of reported performance measures.

Performance measure	Description
t_r	Travel time in the rock [y].
U_r	Initial Darcy flux in the rock [m/y].
L_r	Path length in the rock [m].
F_r	Flow-related transport resistance in the rock [y/m].
t_t	Travel time in the tunnels [y].
U_t	Initial Darcy flux in the tunnels [m/y].
L_t	Path length in the tunnels [m].
t_{EDZ}	Travel time in the EDZ [y].
U_{EDZ}	Initial Darcy flux in the EDZ [m/y].
L_{EDZ}	Length in the EDZ [m].

Table 2-3 to Table 2-6 show the performance measure statistics in the rock, in the tunnels and in the EDZ for the base case.

Cumulative distribution plots for the base case performance measures in the rock are given in Figure 2-4 to Figure 2-6. Histograms of the path lengths in the tunnels and EDZ are given in Figure 2-8 and Figure 2-9.

Cumulative distribution plots (CDF) of performance measures show the cumulative fraction of particles as a function of performance measure value. These plots allow the distribution of performance measure values to be readily seen, including the tails of those distributions. The curves begin (intercept the fraction axis) at the fraction of particles that do not start (due to no fracture being present). In addition, for advective travel time, path length and flow-related transport resistance, the plots end at one minus the fraction of particles that become stuck along the path. The "Fraction OK" row in the performance measure summary statistics tables gives the fraction of particles that are included in the corresponding CDF curves, i.e. one minus the fraction of particles that do not start and the fraction of particles that get stuck for travel time, path length and flow-related transport resistance and one minus the fraction of particles that do not start for initial Darcy flux. For statistics in the tunnels and EDZ the "Fraction OK" is additionally reduced by the fraction of particles that do not enter the tunnels or EDZ respectively.

Table 2-3. Summary statistics for travel-time in the rock and for initial Darcy flux for the base case of the amalgamated repository-scale and regional-scale DFN models. For release time 2020 AD, three paths Q1, Q2, and Q3 were tracked for each of 7,483 release locations in the amalgamated model.

	$Log_{10}(t_r)$ [y]			$Log_{10}(U)$ [m/y]		
	Q1	Q2	Q3	Q1	Q2	Q3
Mean	1.768	1.712	1.740	–3.666	–3.440	–3.984
Median	1.774	1.745	1.783	–3.604	–3.355	–3.954
5th percentile	0.787	0.716	0.749	–5.761	–4.695	–5.889
10th percentile	0.975	0.888	0.922	–5.351	–4.216	–5.425
25th percentile	1.364	1.306	1.332	–4.522	–3.738	–4.694
75th percentile	2.167	2.125	2.152	–2.888	–3.017	–3.326
90th percentile	2.504	2.404	2.439	–2.149	–2.747	–2.697
95th percentile	2.717	2.612	2.642	–1.582	–2.597	–2.023
Std deviation	0.591	0.582	0.580	1.303	0.651	1.183
Variance	0.349	0.339	0.336	1.697	0.424	1.399
Max value	4.737	4.523	3.732	1.937	–0.688	0.589
Min value	–0.140	–0.072	–0.109	–8.503	–6.774	–8.867
Fraction OK	0.565	0.753	0.788	0.663	0.945	1.000

Table 2-4. Summary statistics for path-length and flow-related transport resistance in the rock for the base case of the amalgamated repository-scale and regional-scale DFN models. For release time 2020 AD, three paths Q1, Q2, and Q3 were tracked for each of 7,483 release locations in the amalgamated model.

	$Log_{10}(L_r)$ [m]			$Log_{10}(F_r)$ [y/m]		
	Q1	Q2	Q3	Q1	Q2	Q3
Mean	3.187	3.209	3.211	5.638	5.467	5.578
Median	3.137	3.150	3.155	5.691	5.555	5.652
5^{th} percentile	2.933	2.930	2.925	3.938	3.782	4.010
10^{th} percentile	2.980	2.975	2.976	4.463	4.356	4.490
25^{th} percentile	3.050	3.051	3.055	5.128	5.039	5.159
75^{th} percentile	3.303	3.373	3.375	6.232	6.015	6.125
90^{th} percentile	3.487	3.530	3.526	6.716	6.427	6.542
95^{th} percentile	3.550	3.588	3.583	7.080	6.682	6.825
Std deviation	0.194	0.214	0.212	0.930	0.867	0.860
Variance	0.038	0.046	0.045	0.866	0.751	0.740
Max value	4.125	4.199	4.303	9.405	9.404	9.404
Min value	2.774	2.760	2.780	2.445	2.387	2.301
Fraction OK	0.565	0.753	0.788	0.565	0.753	0.788

Table 2-5. Summary statistics for travel-time and path-length in the tunnels for the base case of the amalgamated repository-scale and regional-scale DFN models. For release time 2020 AD, three paths Q1, Q2, and Q3 were tracked for each of 7,483 release locations in the amalgamated model.

	$Log_{10}(t_t)$ [y]			$Log_{10}(L_t)$ [m]		
	Q1	Q2	Q3	Q1	Q2	Q3
Mean	5.080	4.896	5.439	1.165	1.116	1.279
Median	5.207	5.046	5.414	1.176	1.105	1.243
5th percentile	3.292	3.079	4.329	0.294	0.179	0.673
10th percentile	3.790	3.442	4.561	0.510	0.408	0.793
25th percentile	4.485	4.176	4.941	0.871	0.774	0.969
75th percentile	5.768	5.659	5.907	1.484	1.485	1.538
90th percentile	6.194	6.089	6.340	1.775	1.794	1.826
95th percentile	6.418	6.332	6.648	1.959	1.981	1.992
Std deviation	0.968	1.033	0.713	0.515	0.561	0.427
Variance	0.938	1.067	0.509	0.265	0.314	0.182
Max value	7.762	8.957	9.138	2.882	2.901	2.893
Min value	–0.387	1.340	3.128	–0.853	–0.905	0.161
Fraction OK	0.408	0.633	0.788	0.408	0.633	0.788

Table 2-6. Summary statistics for travel-time and path-length in the EDZ for the base case of the amalgamated repository-scale and regional-scale DFN models. For release time 2020 AD, three paths Q1, Q2, and Q3 were tracked for each of 7,483 release locations in the amalgamated model.

	$Log_{10}(t_{EDZ})$ [y]			$Log_{10}(L_{EDZ})$ [m]		
	Q1	Q2	Q3	Q1	Q2	Q3
Mean	–0.313	–0.197	–0.151	1.266	1.354	1.528
Median	–0.268	–0.221	–0.103	1.329	1.411	1.598
5th percentile	–1.721	–1.813	–1.885	0.199	0.060	0.440
10th percentile	–1.323	–1.395	–1.467	0.532	0.404	0.744
25th percentile	–0.760	–0.774	–0.739	0.935	0.903	1.149
75th percentile	0.202	0.326	0.407	1.633	1.839	1.972
90th percentile	0.631	0.905	0.860	1.893	2.189	2.261
95th percentile	0.858	1.833	1.487	2.052	2.315	2.362
Std deviation	0.781	0.991	1.012	0.527	0.647	0.590
Variance	0.610	0.981	1.025	0.278	0.418	0.349
Max value	2.032	3.663	3.919	2.486	2.981	3.119
Min value	–4.323	–4.749	–4.325	–0.445	–0.900	–0.540
Fraction OK	0.297	0.753	0.466	0.297	0.753	0.466

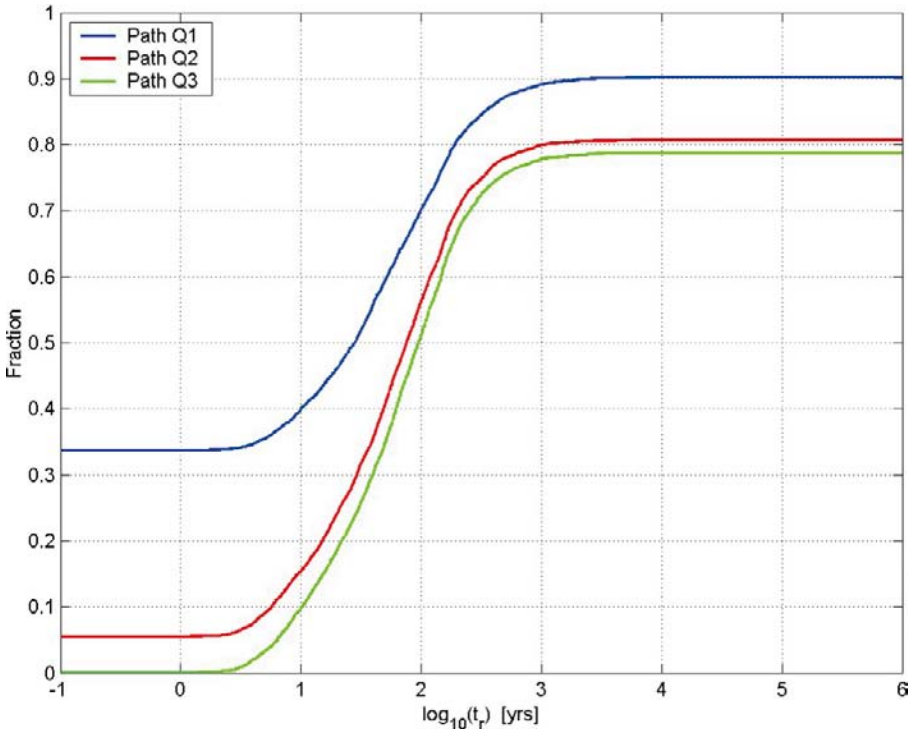

Figure 2-4. *Cumulative distribution plots of travel-time in the rock, t_r, for paths Q1, Q2 and Q3 in the base case of the amalgamated repository-scale and regional-scale DFN models with 7,483 particles released at time 2020 AD.*

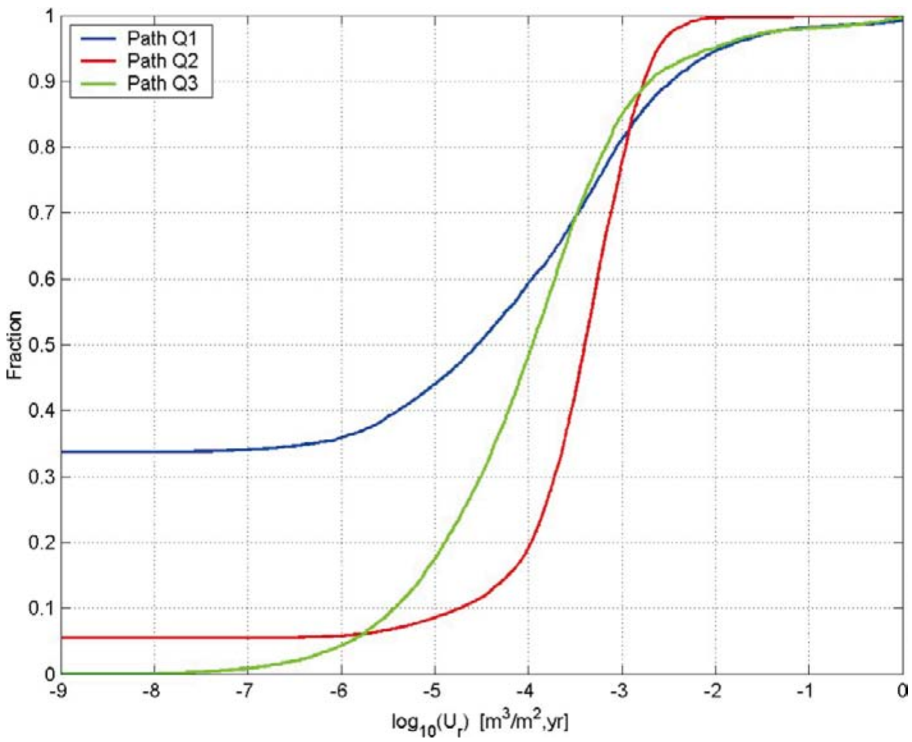

Figure 2-5. *Cumulative distribution plots of initial Darcy flux, U, for paths Q1, Q2 and Q3 in the base case of the amalgamated repository-scale and regional-scale DFN models with 7,483 particles released at time 2020 AD.*

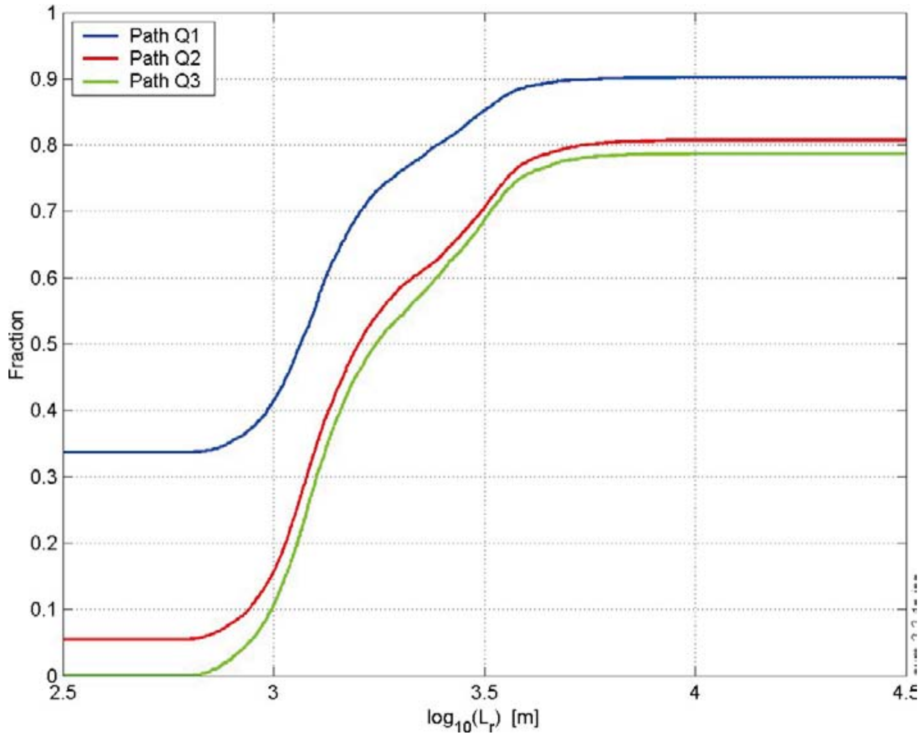

Figure 2-6. *Cumulative distribution plot of path-length in the rock, L_r, for paths Q1, Q2 and Q3 in the base case of the amalgamated repository-scale and regional-scale DFN models with 7,483 particles released at time 2020 AD.*

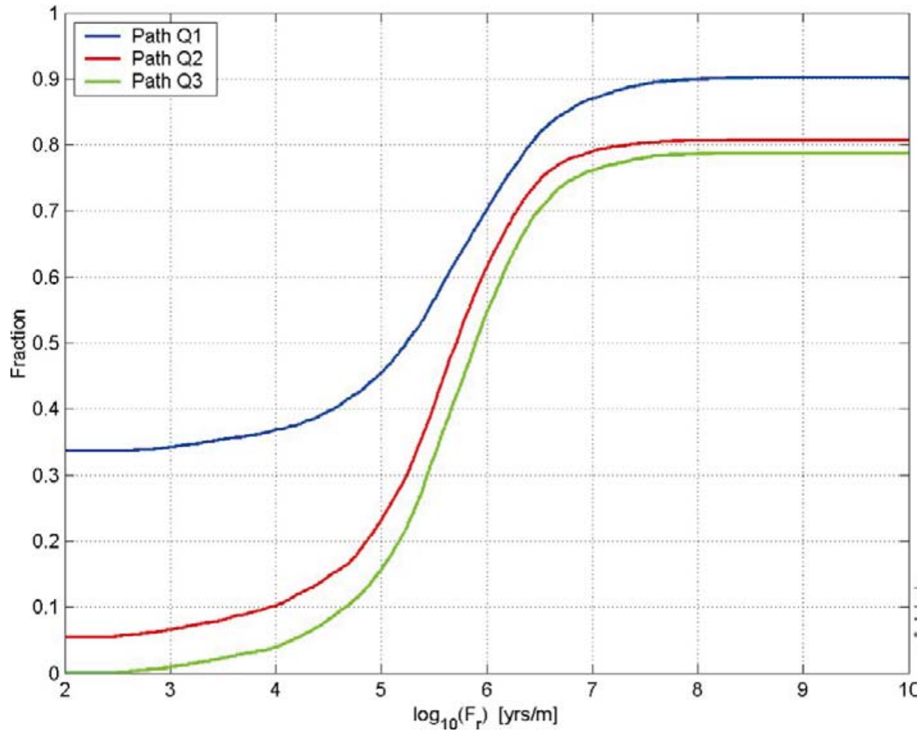

Figure 2-7. *Cumulative distribution plots of flow-related transport resistance in the rock, F_r, for paths Q1, Q2 and Q3 in the base case of the amalgamated repository-scale and regional-scale DFN models with 7,483 particles released at time 2020 AD.*

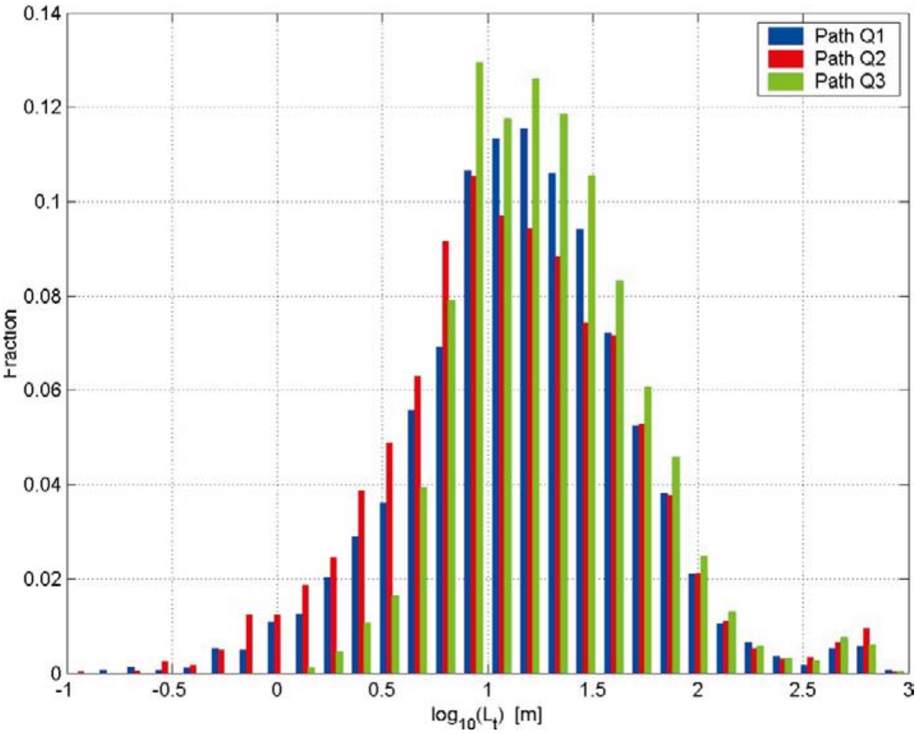

Figure 2-8. *Histograms of path-length in the tunnel, L_t, for paths Q1, Q2 and Q3 in the base case of the amalgamated repository-scale and regional-scale DFN models with 7,483 particles released at time 2020 AD.*

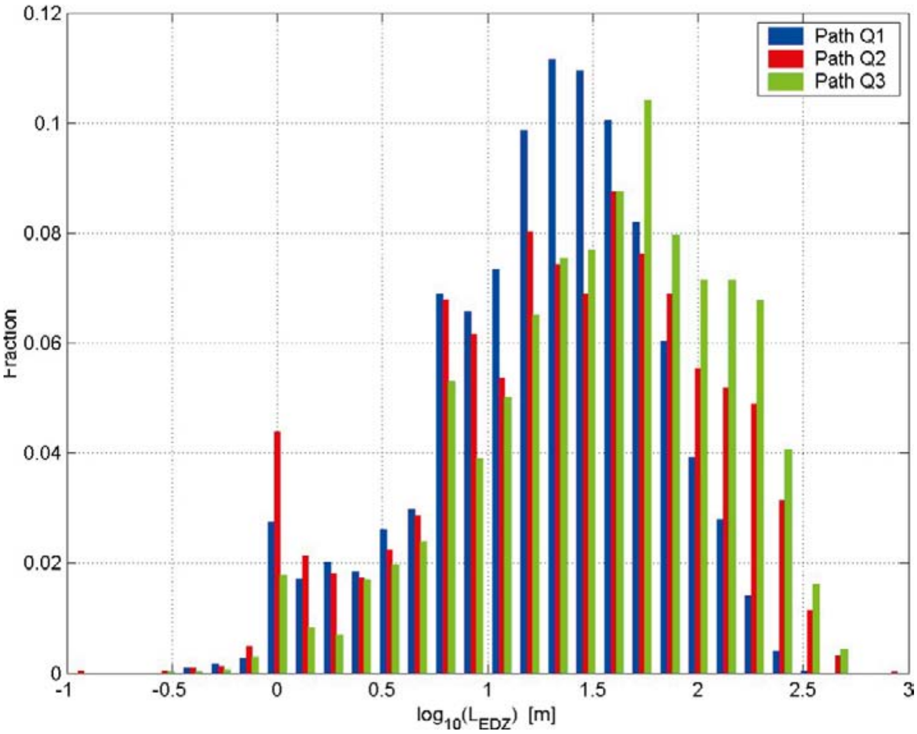

Figure 2-9. *Histograms of path-length in the EDZ, L_{EDZ}, for paths Q1, Q2 and Q3 in the base case of the amalgamated repository-scale and regional-scale DFN models with 7,483 particles released at time 2020 AD.*

Particles released from the top surface

To study whether or not there were any flow pathways from the surface to the repository, 5,261 particles were released above the top surface of the regional DFN model region at an elevation of 0.0 m and with a spacing of 100 m.

Figure 2-10 shows the pathlines for these particles. Most particles remained close to the top surface but a few penetrated to repository depth, as shown in Figure 2-11. Only two particles entered repository features and that was at the upper part of the ramp, close to where they started, and only remained in the ramp for a short length. Figure 2-12 shows one of these particles.

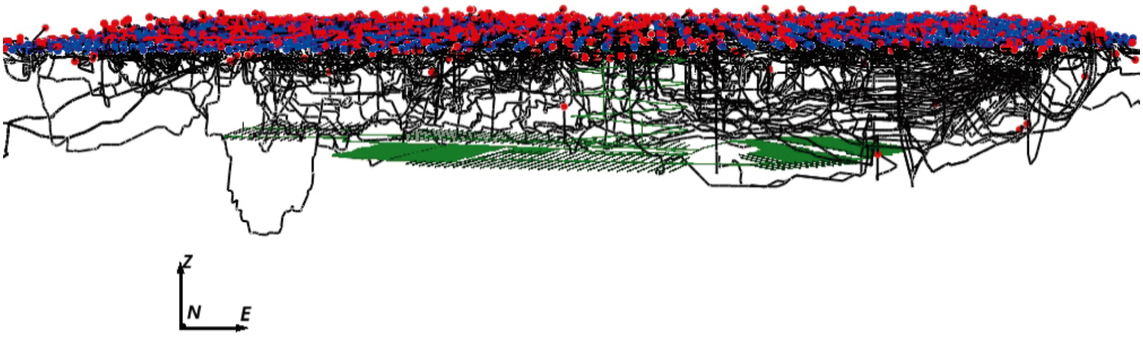

Figure 2-10. Paths released from the top surface in the base case of the amalgamated repository-scale and regional-scale DFN models with 5,261 particles released at time 2020 AD. Start points are coloured blue, end points are coloured red and pathlines are coloured black. The repository features are coloured green. Fractures and rock have been removed.

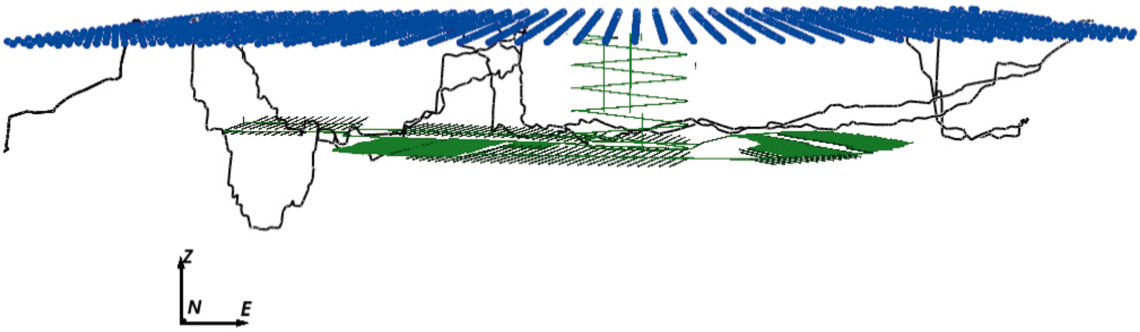

Figure 2-11. Paths released from the top surface and reaching repository depths in the base case of the amalgamated repository-scale and regional-scale DFN models with 5,261 particles released at time 2020 AD. Start points are coloured blue and pathlines are coloured black. The repository features are coloured green. Fractures and rock have been removed.

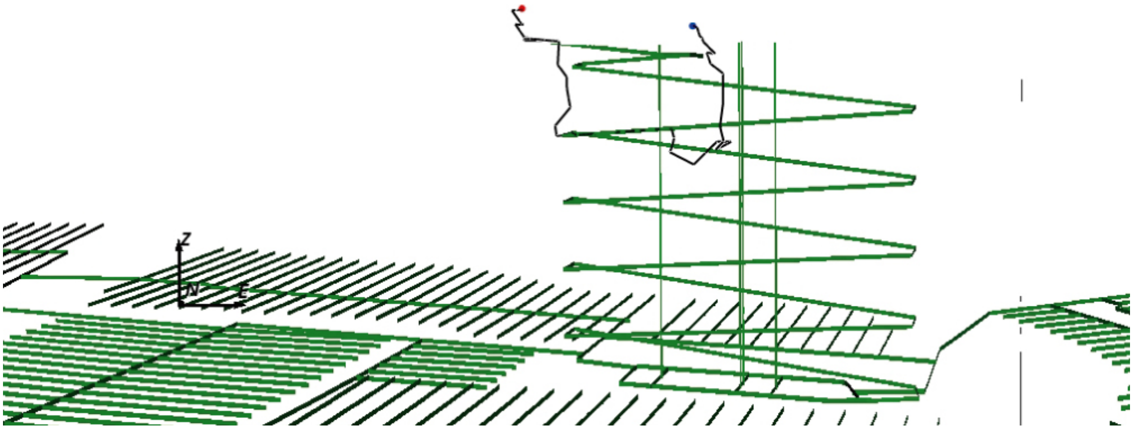

Figure 2-12. A path released from the top surface and entering the ramp in the base case of the amalgamated repository-scale and regional-scale DFN models with 5,261 particles released at time 2020 AD. Start points are coloured blue, end points are coloured red and pathlines are coloured black. The repository features are coloured green. Fractures and rock have been removed.

2.3 Laxemar degraded tunnel backfill variant

This variant model takes the base case from Section 2.2 and increases the hydraulic conductivity of the main, transport and deposition tunnels from 10^{-10} m/s to 10^{-8} m/s.

Table 2-7 to Table 2-10 show the performance measure statistics in the rock, the tunnels and the EDZ for this variant case. Comparison to Table 2-3 to Table 2-6 for the base case show that there is a minor decrease in mean travel time and path length, a minor increase in mean initial Darcy flux and a decrease in mean flow-related transport resistance in the rock. There is an increase in the mean path lengths in the tunnels for this variant case and a decrease in the mean time in the tunnels. There is a minor decrease in the mean path lengths and travel times in the EDZ. The histogram in Figure 2-13 shows more paths with longer lengths in the tunnels for the variant compared to the base case shown in Figure 2-8. The histogram in Figure 2-14 shows fewer paths with longer lengths in the EDZ for the variant compared to the base case shown in Figure 2-9.

The results indicate that there was a greater flow in the tunnels for this variant compared to the base case due to the higher hydraulic conductivity. This drew more particles into the tunnels where they travelled with a higher velocity. The effects were particularly strong for the Q3 particles because they started in the tunnels.

Table 2-7. Summary statistics for travel-time in the rock and for initial Darcy flux for the degraded tunnel backfill variant case of the amalgamated repository-scale and regional-scale DFN models. For release time 2020 AD, three paths Q1, Q2, and Q3 were tracked for each of 7,483 release locations in the amalgamated model.

	$Log_{10}(t_r)$ [y]			$Log_{10}(U)$ [m/y]		
	Q1	Q2	Q3	Q1	Q2	Q3
Mean	1.676	1.601	1.575	–3.533	–3.399	–3.452
Median	1.671	1.647	1.604	–3.484	–3.305	–3.447
5th percentile	0.733	0.646	0.622	–5.560	–4.551	–5.437
10th percentile	0.896	0.800	0.770	–5.158	–4.176	–4.814
25th percentile	1.258	1.137	1.109	–4.415	–3.687	–4.031
75th percentile	2.100	2.019	2.004	–2.725	–2.986	–2.893
90th percentile	2.396	2.307	2.312	–2.049	–2.771	–2.135
95th percentile	2.623	2.538	2.550	–1.551	–2.638	–1.571
Std deviation	0.582	0.588	0.597	1.268	0.609	1.158
Variance	0.338	0.345	0.357	1.608	0.371	1.342
Max value	4.634	4.409	3.901	1.938	–0.720	0.891
Min value	–0.094	–0.150	–0.044	–7.767	–6.347	–9.503
Fraction OK	0.528	0.674	0.695	0.658	0.922	0.987

Table 2-8. Summary statistics for path-length and flow-related transport resistance in the rock for the degraded tunnel backfill variant case of the amalgamated repository-scale and regional-scale DFN models. For release time 2020 AD, three paths Q1, Q2, and Q3 were tracked for each of 7,483 release locations in the amalgamated model.

	$Log_{10}(L_r)$ [m]			$Log_{10}(F_r)$ [y/m]		
	Q1	Q2	Q3	Q1	Q2	Q3
Mean	3.176	3.187	3.179	5.418	5.192	5.151
Median	3.124	3.128	3.121	5.454	5.282	5.268
5th percentile	2.927	2.919	2.914	3.847	3.575	3.468
10th percentile	2.975	2.963	2.957	4.325	4.072	3.977
25th percentile	3.044	3.037	3.033	4.930	4.765	4.696
75th percentile	3.285	3.331	3.309	5.962	5.711	5.698
90th percentile	3.481	3.513	3.508	6.443	6.129	6.103
95th percentile	3.545	3.572	3.553	6.766	6.408	6.374
Std deviation	0.192	0.209	0.203	0.873	0.835	0.863
Variance	0.037	0.044	0.041	0.762	0.698	0.744
Max value	4.125	4.246	3.981	9.130	8.742	9.079
Min value	2.773	2.770	2.775	2.182	2.365	2.346
Fraction OK	0.528	0.674	0.695	0.528	0.674	0.695

Table 2-9. Summary statistics for travel-time and path-length in the tunnels for the degraded tunnel backfill variant case of the amalgamated repository-scale and regional-scale DFN models. For release time 2020 AD, three paths Q1, Q2, and Q3 were tracked for each of 7,483 release locations in the amalgamated model.

	$Log_{10}(t_t)$ [y]			$Log_{10}(L_t)$ [m]		
	Q1	Q2	Q3	Q1	Q2	Q3
Mean	4.614	4.769	4.336	1.328	1.349	1.475
Median	4.753	4.909	4.204	1.368	1.390	1.493
5th percentile	2.360	2.636	2.831	0.419	0.405	0.724
10th percentile	3.098	3.387	3.112	0.668	0.639	0.860
25th percentile	3.921	4.127	3.630	0.999	0.960	1.147
75th percentile	5.501	5.617	5.015	1.698	1.742	1.796
90th percentile	6.023	6.083	5.801	1.921	1.980	2.021
95th percentile	6.312	6.331	6.182	2.029	2.164	2.176
Std deviation	1.225	1.175	1.015	0.515	0.550	0.460
Variance	1.499	1.381	1.031	0.265	0.303	0.212
Max value	7.355	7.754	7.874	2.896	3.035	3.256
Min value	–0.138	–0.081	1.627	–0.660	–0.704	0.173
Fraction OK	0.404	0.582	0.695	0.404	0.582	0.695

Table 2-10. Summary statistics for travel-time and path-length in the EDZ for the degraded tunnel backfill variant case of the amalgamated repository-scale and regional-scale DFN models. For release time 2020 AD, three paths Q1, Q2, and Q3 were tracked for each of 7,483 release locations in the amalgamated model.

	$Log_{10}(t_{EDZ})$ [y]			$Log_{10}(L_{EDZ})$ [m]		
	Q1	Q2	Q3	Q1	Q2	Q3
Mean	–0.431	–0.294	–0.592	1.181	1.317	1.330
Median	–0.406	–0.323	–0.457	1.202	1.325	1.427
5th percentile	–1.755	–1.709	–2.511	0.301	0.196	0.028
10th percentile	–1.334	–1.324	–2.210	0.554	0.512	0.451
25th percentile	–0.869	–0.794	–1.283	0.833	0.860	0.902
75th percentile	0.048	0.163	0.120	1.529	1.757	1.823
90th percentile	0.439	0.655	0.620	1.777	2.114	2.154
95th percentile	0.749	1.316	1.075	1.927	2.289	2.330
Std deviation	0.738	0.862	1.112	0.491	0.617	0.729
Variance	0.544	0.744	1.237	0.241	0.381	0.532
Max value	2.066	2.849	2.967	2.468	3.304	3.363
Min value	–2.944	–5.010	–4.467	–1.211	–0.830	–1.028
Fraction OK	0.254	0.674	0.314	0.254	0.674	0.314

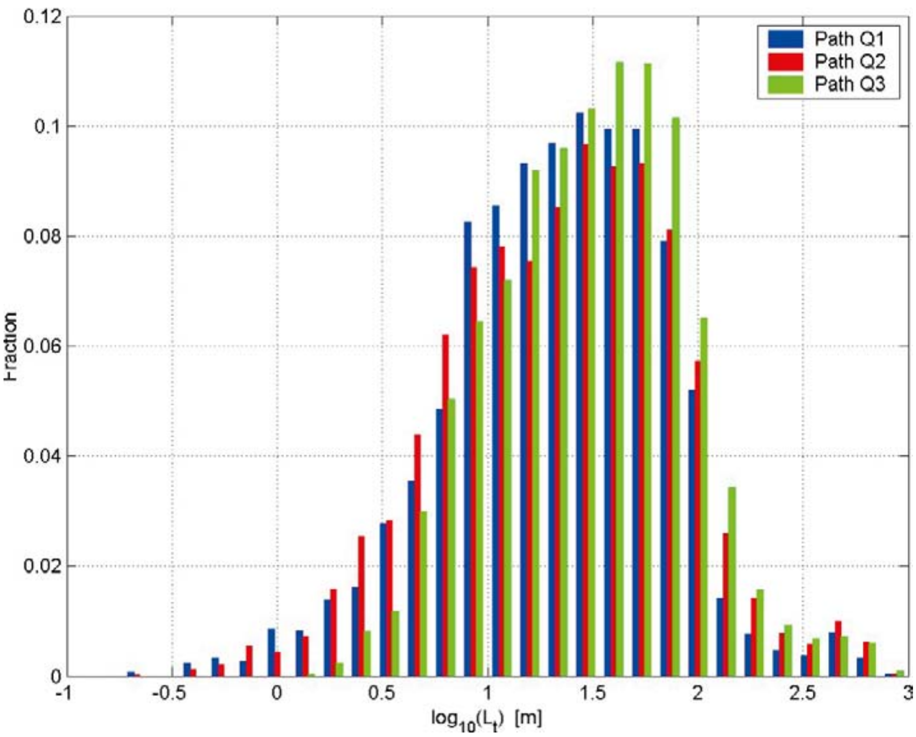

Figure 2-13. *Histograms of path-length in the tunnel, L_t, for paths Q1, Q2 and Q3 in the degraded tunnel backfill variant of the amalgamated repository-scale and regional-scale DFN models with 7,483 particles released at time 2020 AD.*

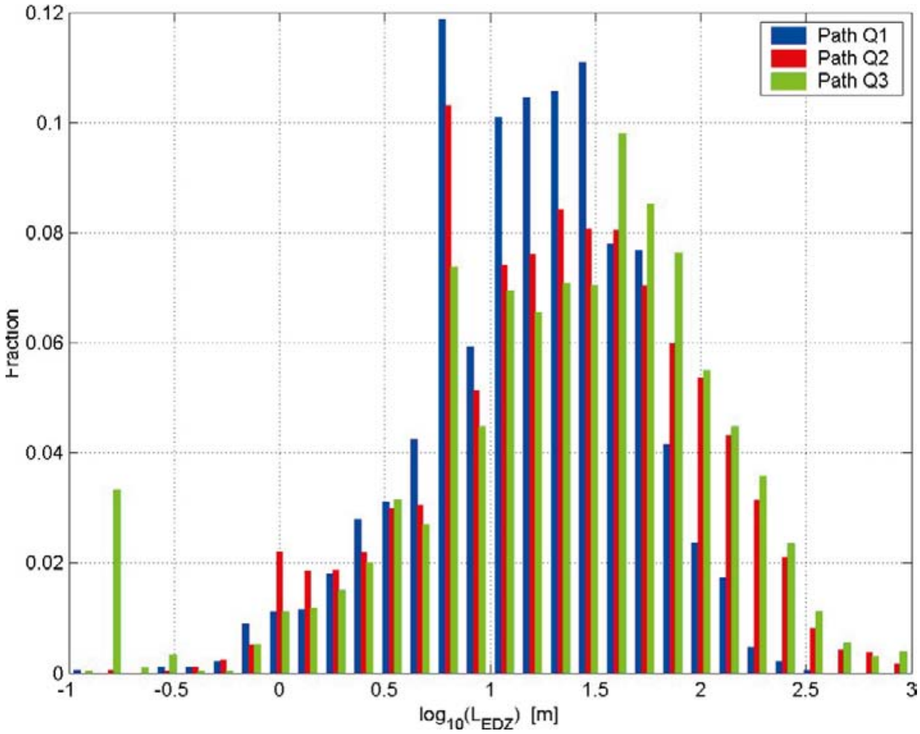

Figure 2-14. *Histograms of path-length in the EDZ, L_{EDZ}, for paths Q1, Q2 and Q3 in the degraded tunnel backfill variant of the amalgamated repository-scale and regional-scale DFN models with 7,483 particles released at time 2020 AD.*

2.4 Laxemar enhanced central area, ramp and shaft backfill variant

This variant model takes the base case from Section 2.2 and reduces the hydraulic conductivity of the central area, ramp and shaft backfill from 10^{-5} m/s to 10^{-8} m/s.

Table 2-11 to Table 2-14 show the performance measure statistics in the rock, the tunnels and the EDZ for this variant case. Comparison to Table 2-3 to Table 2-6 for the base case shows that there is little difference in the performance measures for the rock. There is a slight decrease in the mean path lengths in the tunnels for the variant case. The histogram in Figure 2-15 shows fewer paths with longer lengths (above 100 m) in the tunnels for the variant compared to the base case shown in Figure 2-8. The histogram in Figure 2-16 shows little difference in path lengths in the EDZ for the variant compared to the base case shown in Figure 2-9.

Table 2-11. Summary statistics for travel-time in the rock and for initial Darcy flux for the enhanced central area, ramp and shaft backfill variant case of the amalgamated repository-scale and regional-scale DFN models. For release time 2020 AD, three paths Q1, Q2, and Q3 were tracked for each of 7,483 release locations in the amalgamated model.

	$Log_{10}(t_r)$ [y]			$Log_{10}(U)$ [m/y]		
	Q1	Q2	Q3	Q1	Q2	Q3
Mean	1.770	1.715	1.730	–3.667	–3.442	–3.983
Median	1.777	1.754	1.770	–3.600	–3.357	–3.947
5th percentile	0.789	0.706	0.736	–5.761	–4.700	–5.948
10th percentile	0.972	0.880	0.910	–5.361	–4.213	–5.447
25th percentile	1.373	1.312	1.337	–4.524	–3.745	–4.674
75th percentile	2.171	2.129	2.140	–2.889	–3.019	–3.327
90th percentile	2.496	2.427	2.426	–2.147	–2.747	–2.694
95th percentile	2.704	2.622	2.623	–1.580	–2.600	–2.048
Std deviation	0.587	0.586	0.575	1.304	0.652	1.188
Variance	0.345	0.343	0.331	1.701	0.425	1.412
Max value	4.207	4.405	3.720	1.937	–0.688	0.665
Min value	–0.140	–0.072	0.000	–8.501	–6.774	–8.920
Fraction OK	0.574	0.756	0.779	0.663	0.945	1.000

Table 2-12. Summary statistics for path-length and flow-related transport resistance in the rock for the enhanced central area, ramp and shaft backfill variant case of the amalgamated repository-scale and regional-scale DFN models. For release time 2020 AD, three paths Q1, Q2, and Q3 were tracked for each of 7,483 release locations in the amalgamated model.

	$Log_{10}(L_r)$ [m]			$Log_{10}(F_r)$ [y/m]		
	Q1	Q2	Q3	Q1	Q2	Q3
Mean	3.183	3.201	3.201	5.642	5.475	5.574
Median	3.139	3.143	3.143	5.705	5.570	5.668
5th percentile	2.928	2.922	2.924	3.896	3.770	3.946
10th percentile	2.978	2.968	2.971	4.503	4.327	4.487
25th percentile	3.051	3.048	3.048	5.147	5.053	5.153
75th percentile	3.291	3.355	3.355	6.229	6.026	6.116
90th percentile	3.479	3.520	3.518	6.705	6.438	6.510
95th percentile	3.545	3.576	3.572	7.022	6.730	6.786
Std deviation	0.191	0.211	0.209	0.923	0.880	0.862
Variance	0.036	0.044	0.044	0.851	0.774	0.743
Max value	4.155	4.249	4.050	9.306	9.406	9.407
Min value	2.796	2.758	2.766	2.212	2.309	2.301
Fraction OK	0.574	0.756	0.779	0.574	0.756	0.779

Table 2-13. Summary statistics for travel-time and path-length in the tunnels for the enhanced central area, ramp and shaft backfill variant case of the amalgamated repository-scale and regional-scale DFN models. For release time 2020 AD, three paths Q1, Q2, and Q3 were tracked for each of 7,483 release locations in the amalgamated model.

	$Log_{10}(t_t)$ [y]			$Log_{10}(L_t)$ [m]		
	Q1	Q2	Q3	Q1	Q2	Q3
Mean	5.085	4.900	5.439	1.151	1.085	1.255
Median	5.233	5.023	5.412	1.171	1.090	1.227
5th percentile	3.286	3.091	4.323	0.269	0.177	0.661
10th percentile	3.764	3.420	4.548	0.519	0.407	0.789
25th percentile	4.490	4.152	4.941	0.876	0.750	0.969
75th percentile	5.777	5.673	5.903	1.486	1.455	1.522
90th percentile	6.187	6.129	6.335	1.759	1.780	1.777
95th percentile	6.430	6.398	6.605	1.905	1.912	1.922
Std deviation	0.963	1.054	0.708	0.490	0.525	0.388
Variance	0.927	1.111	0.501	0.241	0.276	0.151
Max value	7.762	8.988	9.528	2.473	2.887	2.981
Min value	–0.387	1.035	3.127	–0.853	–0.905	0.161
Fraction OK	0.412	0.632	0.779	0.412	0.632	0.779

Table 2-14. Summary statistics for travel-time and path-length in the EDZ for the enhanced central area, ramp and shaft backfill variant case of the amalgamated repository-scale and regional-scale DFN models. For release time 2020 AD, three paths Q1, Q2, and Q3 were tracked for each of 7,483 release locations in the amalgamated model.

	$Log_{10}(t_{EDZ})$ [y]			$Log_{10}(L_{EDZ})$ [m]		
	Q1	Q2	Q3	Q1	Q2	Q3
Mean	–0.301	–0.189	–0.135	1.266	1.338	1.518
Median	–0.249	–0.213	–0.113	1.329	1.385	1.580
5th percentile	–1.652	–1.824	–1.896	0.254	0.060	0.456
10th percentile	–1.286	–1.413	–1.396	0.542	0.415	0.760
25th percentile	–0.750	–0.768	–0.686	0.926	0.904	1.152
75th percentile	0.200	0.334	0.409	1.644	1.814	1.943
90th percentile	0.614	0.910	0.887	1.888	2.162	2.246
95th percentile	0.853	1.937	1.485	2.043	2.285	2.348
Std deviation	0.768	1.010	1.010	0.525	0.635	0.578
Variance	0.590	1.019	1.021	0.275	0.404	0.334
Max value	2.126	4.095	4.525	2.495	2.797	3.107
Min value	–4.789	–4.749	–4.789	–0.560	–0.900	–0.434
Fraction OK	0.301	0.756	0.458	0.301	0.756	0.458

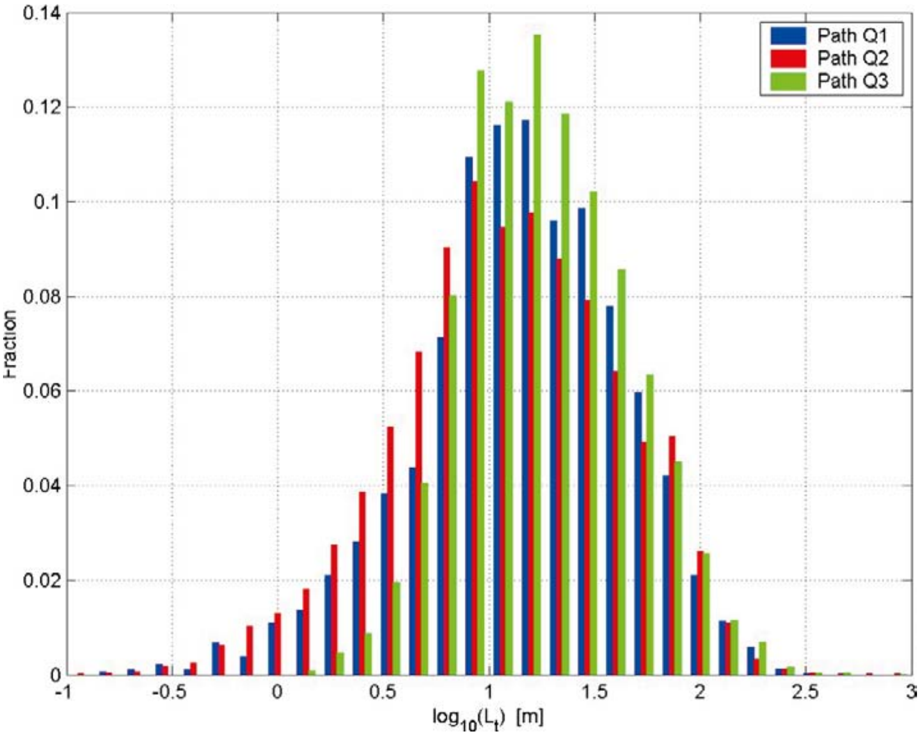

***Figure 2-15.** Histograms of path-length in the tunnel, L_t, for paths Q1, Q2 and Q3 in the enhanced central area, ramp and shaft backfill variant of the amalgamated repository-scale and regional-scale DFN models with 7,483 particles released at time 2020 AD.*

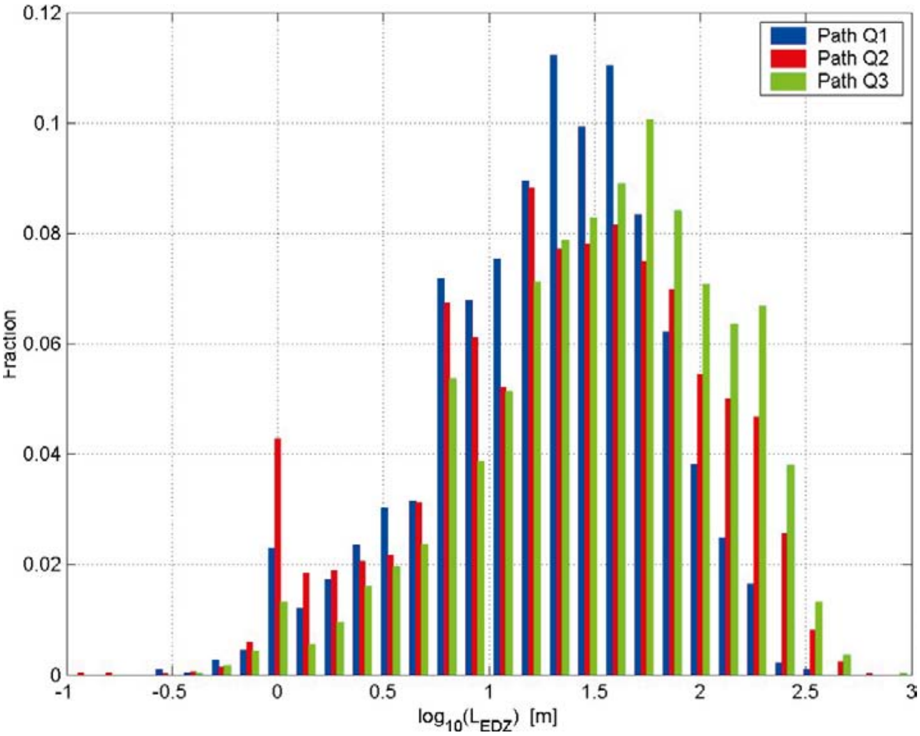

***Figure 2-16.** Histograms of path-length in the EDZ, L_{EDZ}, for paths Q1, Q2 and Q3 in the enhanced central area, ramp and shaft backfill variant of the amalgamated repository-scale and regional-scale DFN models with 7,483 particles released at time 2020 AD.*

3 Sensitivity analysis of crown space and EDZ

3.1 Laxemar crown space base case

This variant model takes the base case from Section 2.2 and adds a crown space to the deposition tunnels. The crown space is a region at the top of tunnels where the backfill has subsided due to consolidation. This was represented in the repository scale model by changing the rock properties of a narrow band, 0.1 m thick, at top of the deposition tunnels to a high hydraulic conductivity of 10^{-3} m/s. At the regional scale it was represented by adding deterministic fractures with equivalent properties, parallel to and cutting the top of the deposition tunnels, much in the same way that the EDZ beneath the tunnels was modelled.

Figure 3-1 shows the release points in the repository in blue and the exit locations at the regional model boundary in red for the crown space base case. Comparison to Figure 2-3 for the base case shows little change in the exit locations for this variant.

Table 3-1 to Table 3-4 show the performance measure statistics in the rock, the tunnels and the EDZ for this case. Comparison to Table 2-3 to Table 2-6 for the base case show that there is a reduction in the time, length and flow-related transport resistance in the rock. There is an increase in the mean path lengths and a reduction in the travel time in the tunnels for the variant case. There is a reduction in the mean time spent in the EDZ for the variant model paths and an increase in the mean length in the EDZ for Q1 and Q2 paths, but a reduction for Q3. The cumulative distribution function plots in Figure 3-2, Figure 3-4 and Figure 3-5 show a decrease in the proportion of paths with higher values for travel time, path length and flow-related transport resistance respectively in the rock compared to the corresponding plots for the base case in Figure 2-4, Figure 2-6 and Figure 2-7. The cumulative distribution function plot in Figure 3-3 shows some minor changes in the distribution of initial Darcy velocities in the rock compared to the corresponding base case plot in Figure 2-5. The histogram

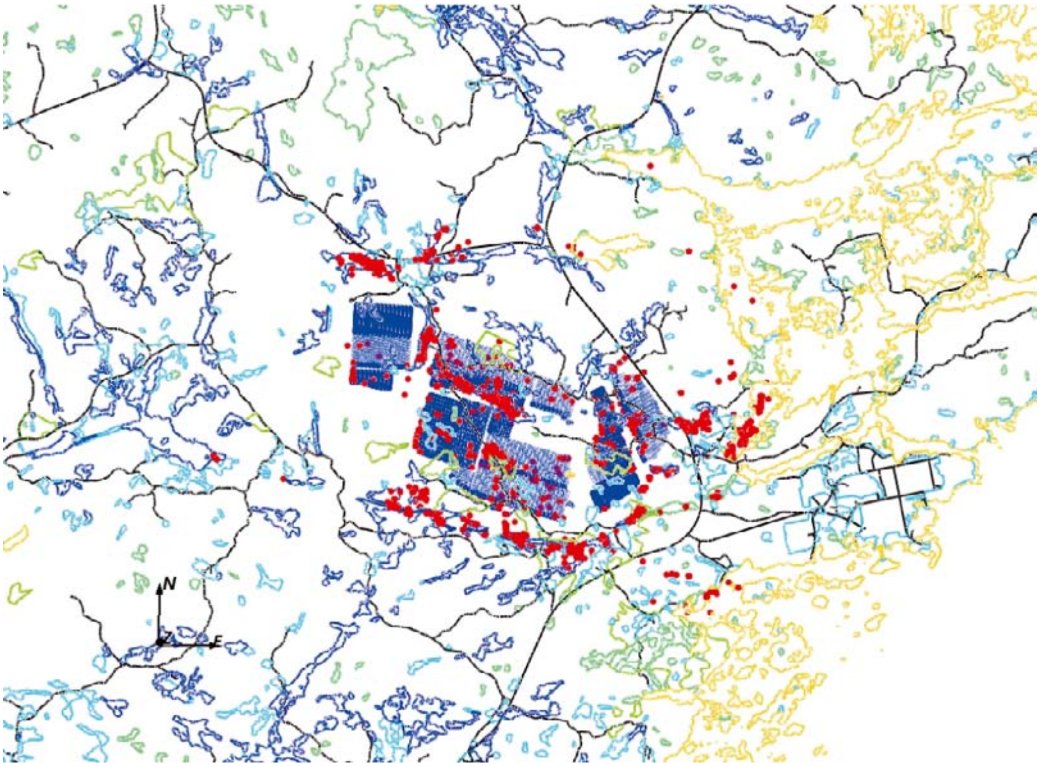

Figure 3-1. Particle release and exit points viewed from above, for paths Q1, Q2 and Q3 in the crown space base case of the amalgamated repository-scale and regional-scale DFN models with 7,483 particles released at time 2020 AD. Release points are coloured blue and exit locations are coloured red.

in Figure 3-6 shows a greater proportion of paths with longer lengths in the tunnels for this variant compared to the base case shown in Figure 2-8. The histogram in Figure 3-7 also shows a greater proportion of paths with longer lengths in the EDZ for this variant compared to the base case shown in Figure 2-9.

These results suggest that particles were being pulled into the tunnels by the presence of the crown space and had a greater proportion of their path lengths there. The reduction in the time spent in the tunnels was because the particles were travelling down the high permeability crown space with an increased velocity. Figure 3-8 shows the pathlines along the crown space of a deposition tunnel. The Darcy flux in the crown space was greater than the rest of the tunnel due to the higher hydraulic conductivity.

There was less effect on the travel time in the tunnels for the Q3 release locations compared to the base case because these particles needed to travel through the low permeability backfill in the tunnel in order to reach the crown space. However, the Q1 and Q2 particles could reach the crown space via alternative pathways through the fracture system. In all cases, particles must leave the crown space above the deposition tunnels before a main tunnel is reached because main tunnels had not been modelled with a crown space.

Table 3-1. Summary statistics for travel-time in the rock and for initial Darcy flux for the crown space base case of the amalgamated repository-scale and regional-scale DFN models. For release time 2020 AD, three paths Q1, Q2, and Q3 were tracked for each of 7,483 release locations in the amalgamated model.

	$Log_{10}(t_r)$ [y]			$Log_{10}(U)$ [m/y]		
	Q1	Q2	Q3	Q1	Q2	Q3
Mean	1.708	1.612	1.613	–3.613	–3.570	–3.714
Median	1.713	1.653	1.649	–3.625	–3.550	–3.859
5th percentile	0.679	0.636	0.602	–5.830	–4.690	–5.951
10th percentile	0.834	0.757	0.723	–5.369	–4.439	–5.396
25th percentile	1.263	1.101	1.088	–4.522	–4.008	–4.621
75th percentile	2.154	2.071	2.087	–2.746	–3.114	–2.971
90th percentile	2.494	2.380	2.418	–1.927	–2.713	–1.663
95th percentile	2.746	2.608	2.669	–1.415	–2.503	–0.871
Std deviation	0.637	0.633	0.654	1.362	0.671	1.468
Variance	0.405	0.400	0.428	1.854	0.450	2.154
Max value	5.409	5.119	4.584	0.717	–1.244	0.735
Min value	–0.014	–0.142	–0.139	–7.765	–6.282	–10.071
Fraction OK	0.517	0.664	0.726	0.667	0.930	1.000

Table 3-2. Summary statistics for path-length and flow-related transport resistance in the rock for the crown space base case of the amalgamated repository-scale and regional-scale DFN models. For release time 2020 AD, three paths Q1, Q2, and Q3 were tracked for each of 7,483 release locations in the amalgamated model.

	$Log_{10}(L_r)$ [m]			$Log_{10}(F_r)$ [y/m]		
	Q1	Q2	Q3	Q1	Q2	Q3
Mean	3.173	3.185	3.172	5.477	5.216	5.198
Median	3.115	3.111	3.105	5.514	5.267	5.278
5^{th} percentile	2.915	2.911	2.912	3.745	3.487	3.189
10^{th} percentile	2.964	2.956	2.955	4.204	3.959	3.717
25^{th} percentile	3.031	3.025	3.023	4.854	4.658	4.623
75^{th} percentile	3.295	3.348	3.300	6.093	5.809	5.856
90^{th} percentile	3.492	3.535	3.518	6.708	6.348	6.400
95^{th} percentile	3.554	3.575	3.564	7.059	6.748	6.771
Std deviation	0.202	0.222	0.211	0.990	0.959	1.042
Variance	0.041	0.049	0.045	0.980	0.919	1.086
Max value	4.180	4.473	4.129	9.505	9.211	9.439
Min value	2.795	2.755	2.761	2.245	2.288	2.261
Fraction OK	0.517	0.664	0.726	0.517	0.664	0.726

Table 3-3. Summary statistics for travel-time and path-length in the tunnels for the crown space base case of the amalgamated repository-scale and regional-scale DFN models. For release time 2020 AD, three paths Q1, Q2, and Q3 were tracked for each of 7,483 release locations in the amalgamated model.

	$Log_{10}(t_t)$ [y]			$Log_{10}(L_t)$ [m]		
	Q1	Q2	Q3	Q1	Q2	Q3
Mean	4.676	4.006	5.437	1.679	1.635	1.725
Median	5.001	4.480	5.444	1.745	1.641	1.760
5th percentile	1.504	–0.642	4.130	0.560	0.613	0.818
10th percentile	2.752	0.657	4.418	0.815	0.832	0.936
25th percentile	4.095	3.101	4.886	1.263	1.168	1.242
75th percentile	5.671	5.440	5.990	2.178	2.169	2.202
90th percentile	6.186	6.062	6.450	2.407	2.428	2.448
95th percentile	6.487	6.412	6.763	2.529	2.546	2.573
Std deviation	1.525	2.029	0.786	0.624	0.618	0.572
Variance	2.325	4.117	0.619	0.389	0.382	0.327
Max value	8.792	9.423	8.740	3.816	3.444	4.012
Min value	–2.483	–3.238	2.987	–0.605	–0.828	0.237
Fraction OK	0.419	0.664	0.726	0.419	0.664	0.726

Table 3-4. Summary statistics for travel-time and path-length in the EDZ for the crown space base case of the amalgamated repository-scale and regional-scale DFN models. For release time 2020 AD, three paths Q1, Q2, and Q3 were tracked for each of 7,483 release locations in the amalgamated model.

	$Log_{10}(t_{EDZ})$ [y]			$Log_{10}(L_{EDZ})$ [m]		
	Q1	Q2	Q3	Q1	Q2	Q3
Mean	–0.925	–0.816	–0.997	1.557	1.578	1.380
Median	–1.011	–0.819	–1.245	1.445	1.712	1.558
5th percentile	–2.597	–2.999	–2.930	1.191	0.247	0.342
10th percentile	–2.340	–2.562	–2.113	1.277	0.834	0.585
25th percentile	–1.790	–1.475	–1.553	1.384	1.370	0.680
75th percentile	–0.057	–0.289	–0.626	1.538	1.892	1.787
90th percentile	0.205	0.605	0.406	2.058	2.261	2.244
95th percentile	0.983	1.767	1.482	2.415	2.325	2.287
Std deviation	1.127	1.288	1.203	0.353	0.576	0.633
Variance	1.269	1.660	1.447	0.124	0.332	0.401
Max value	1.205	4.494	3.834	2.517	2.725	2.712
Min value	–2.670	–4.001	–4.662	1.167	–0.108	0.099
Fraction OK	0.002	0.147	0.105	0.002	0.147	0.105

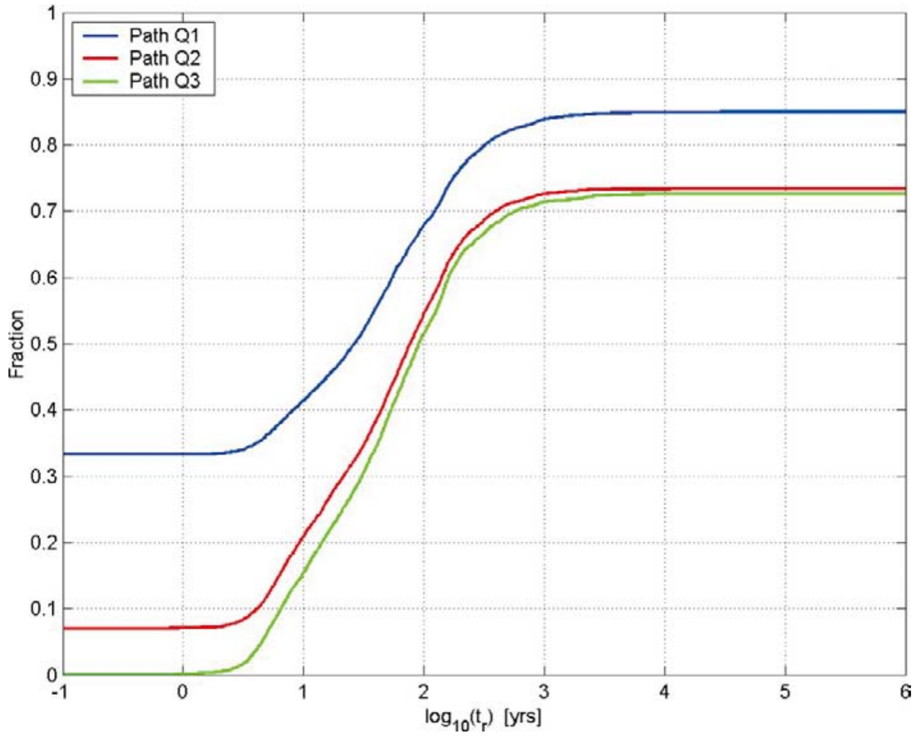

Figure 3-2. *Cumulative distribution plots of travel-time in the rock, t_r, for paths Q1, Q2 and Q3 in the crown space base case of the amalgamated repository-scale and regional-scale DFN models with 7,483 particles released at time 2020 AD.*

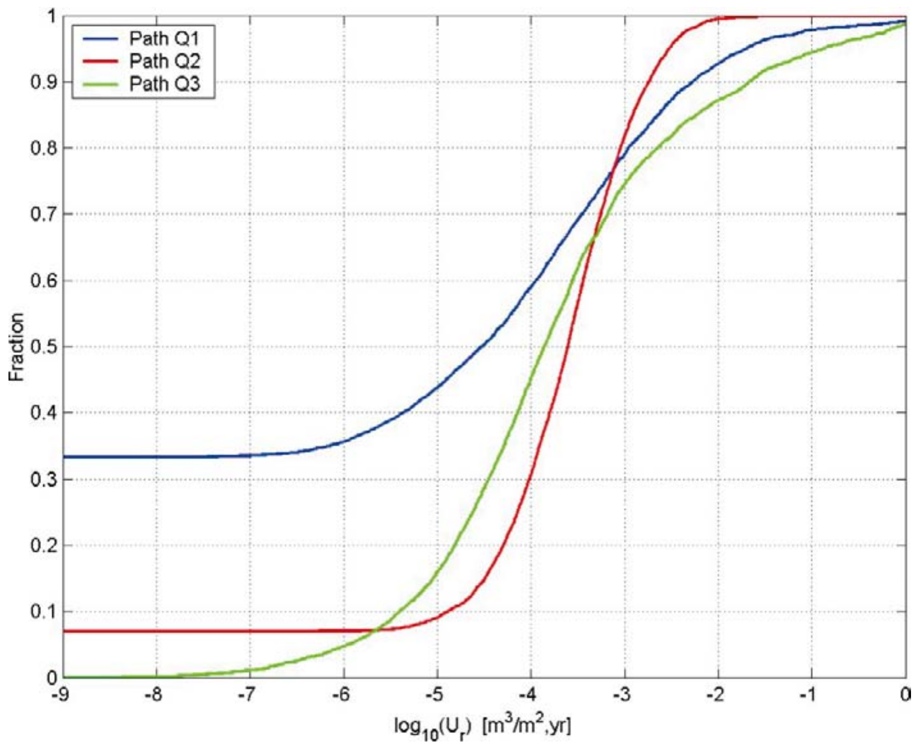

Figure 3-3. *Cumulative distribution plots of initial Darcy flux, U, for paths Q1, Q2 and Q3 in the crown space base case of the amalgamated repository-scale and regional-scale DFN models with 7,483 particles released at time 2020 AD.*

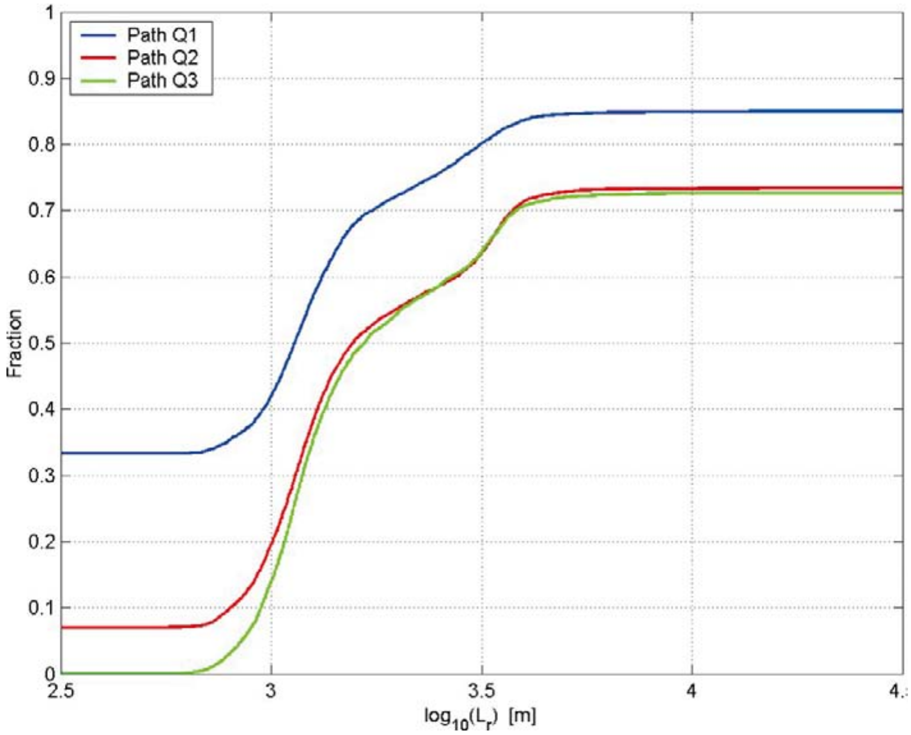

Figure 3-4. *Cumulative distribution plot of path-length in the rock, L_r, for paths Q1, Q2 and Q3 in crown space base case of the amalgamated repository-scale and regional-scale DFN models with 7,483 particles released at time 2020 AD.*

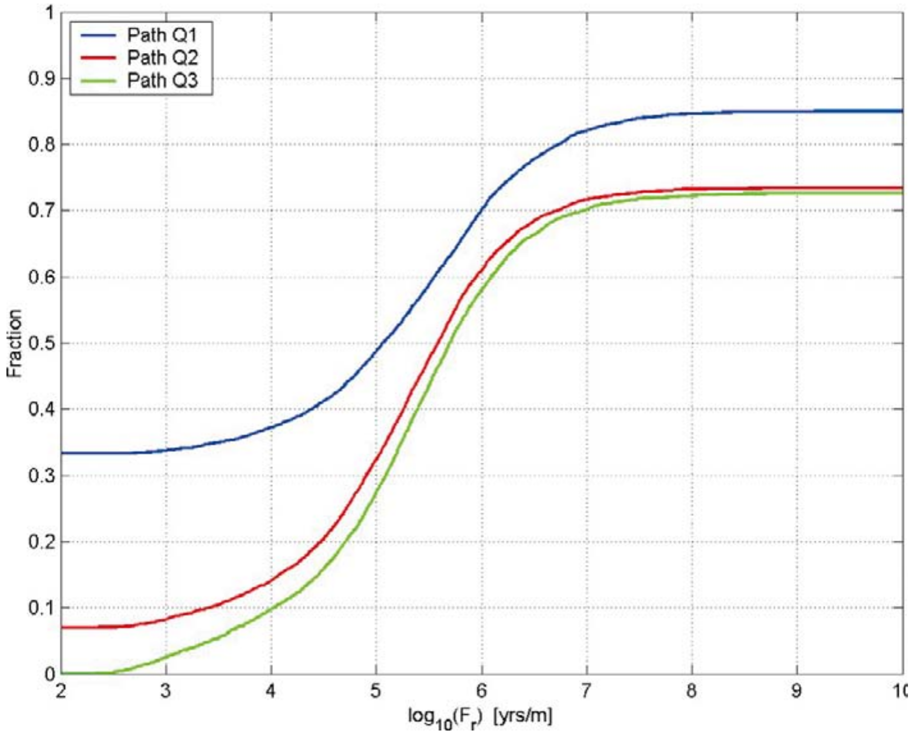

Figure 3-5. *Cumulative distribution plots of flow-related transport resistance in the rock, F_r, for paths Q1, Q2 and Q3 in the crown space base case of the amalgamated repository-scale and regional-scale DFN models with 7,483 particles released at time 2020 AD.*

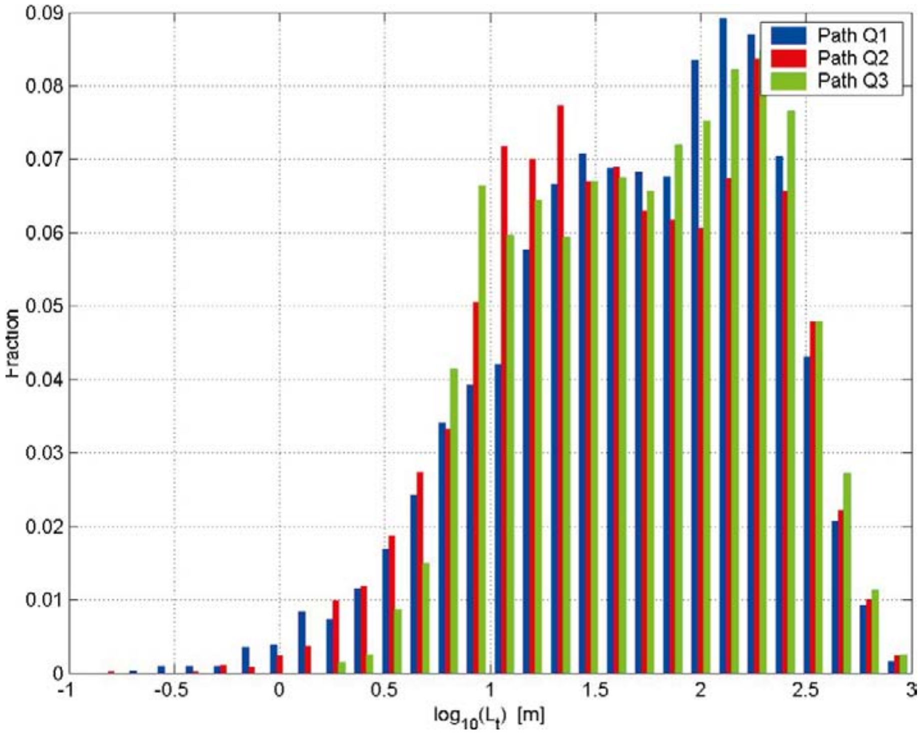

Figure 3-6. *Histograms of path-length in the tunnel, L_t, for paths Q1, Q2 and Q3 in the crown space base case of the amalgamated repository-scale and regional-scale DFN models with 7,483 particles released at time 2020 AD.*

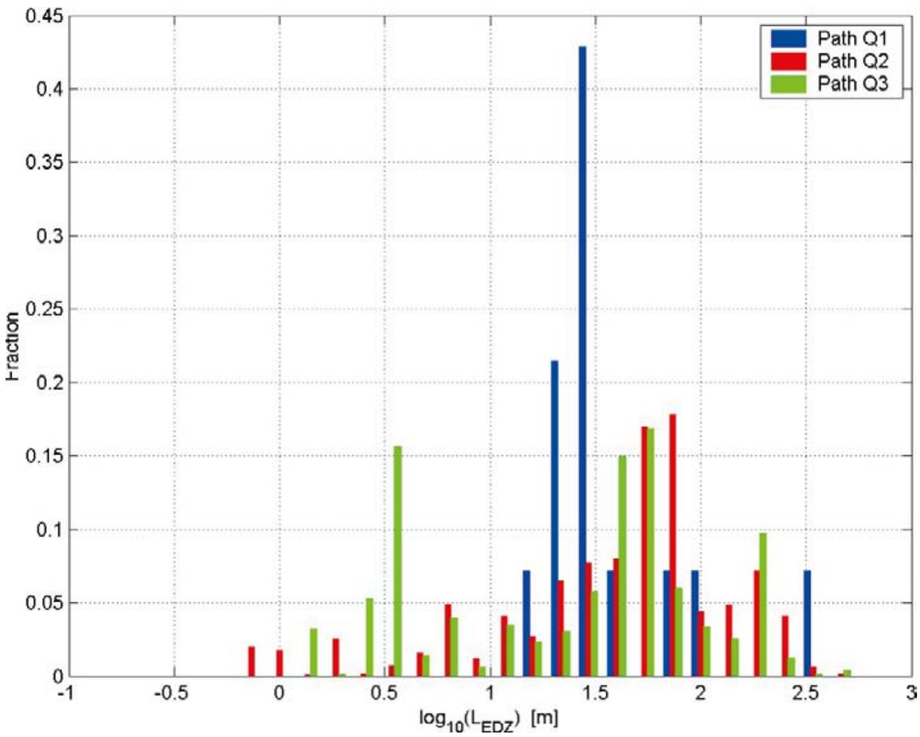

Figure 3-7. *Histograms of path-length in the EDZ, L_{EDZ}, for paths Q1, Q2 and Q3 in the crown space base case of the amalgamated repository-scale and regional-scale DFN models with 7,483 particles released at time 2020 AD.*

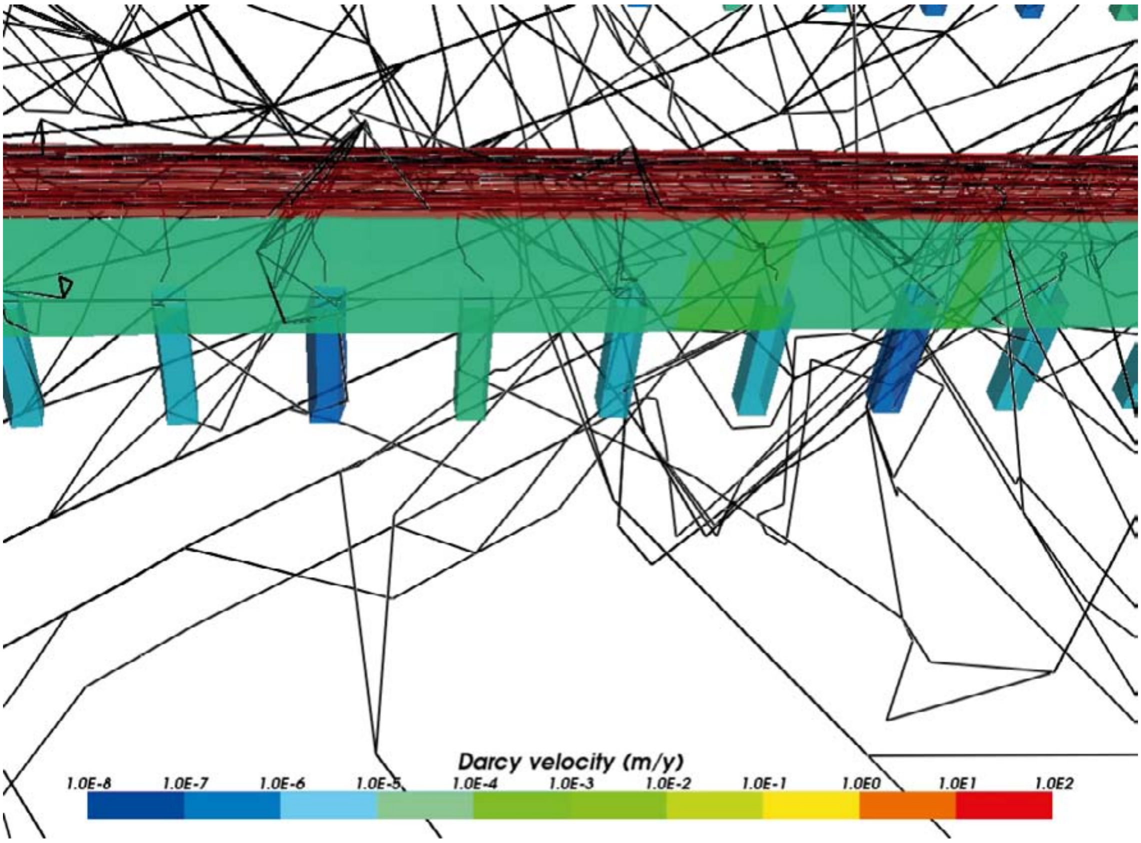

Figure 3-8. *Paths Q1, Q2 and Q3 in the crown space base case of the repository-scale model. Fractures have been removed. The deposition tunnel is coloured by Darcy flux on a log_{10} scale in m/year. The crown space is coloured orange.*

3.2 Laxemar crown space variant with degraded deposition tunnel backfill

This variant model takes the crown space base case from Section 3.1 and increases the hydraulic conductivity of the deposition tunnels from 10^{-10} m/s to 10^{-8} m/s.

Table 3-5 to Table 3-8 show the performance measure statistics in the rock, the tunnels and the EDZ for this variant case. Comparison to Table 3-1 to Table 3-4 for the crown space base case shows that there are minor reductions in the time, length and flow-related transport resistance for the rock. There is also a reduction in the travel time in the tunnels for this variant case and reduction in path lengths for Q2 and Q3 paths, but an increase for Q1. There is a reduction in the mean time spent in the EDZ for the variant model paths and an increase in the mean length in the EDZ for Q1 and Q2 paths, but a reduction for Q3. The histogram in Figure 3-9 shows a similar distribution of path lengths in the tunnels for this variant compared to the crown space base case shown in Figure 3-6. The histogram in Figure 3-10 also shows a similar distribution of path lengths in the EDZ for this variant compared to the crown space base case shown in Figure 3-7.

Table 3-5. Summary statistics for travel-time in the rock and for initial Darcy flux for the crown space, degraded tunnel backfill variant case of the amalgamated repository-scale and regional-scale DFN models. For release time 2020 AD, three paths Q1, Q2, and Q3 were tracked for each of 7,483 release locations in the amalgamated model.

	$Log_{10}(t_r)$ [y]			$Log_{10}(U)$ [m/y]		
	Q1	Q2	Q3	Q1	Q2	Q3
Mean	1.687	1.591	1.584	–3.607	–3.797	–3.677
Median	1.689	1.640	1.624	–3.629	–3.764	–3.857
5th percentile	0.664	0.578	0.581	–5.851	–5.096	–5.833
10th percentile	0.796	0.706	0.697	–5.381	–4.804	–5.409
25th percentile	1.211	1.052	1.049	–4.536	–4.269	–4.639
75th percentile	2.139	2.067	2.051	–2.724	–3.275	–2.871
90th percentile	2.491	2.373	2.364	–1.864	–2.880	–1.571
95th percentile	2.752	2.600	2.610	–1.318	–2.623	–0.737
Std deviation	0.661	0.655	0.655	1.385	0.745	1.496
Variance	0.437	0.429	0.429	1.919	0.555	2.239
Max value	5.125	4.915	4.779	0.748	–1.287	1.164
Min value	–0.091	–0.150	–0.140	–8.242	–7.311	–9.120
Fraction OK	0.499	0.603	0.694	0.662	0.875	1.000

Table 3-6. Summary statistics for path-length and flow-related transport resistance in the rock for the crown space, degraded tunnel backfill variant case of the amalgamated repository-scale and regional-scale DFN models. For release time 2020 AD, three paths Q1, Q2, and Q3 were tracked for each of 7,483 release locations in the amalgamated model.

	$Log_{10}(L_r)$ [m]			$Log_{10}(F_r)$ [y/m]		
	Q1	Q2	Q3	Q1	Q2	Q3
Mean	3.171	3.181	3.180	5.460	5.147	5.105
Median	3.112	3.105	3.108	5.440	5.192	5.178
5^{th} percentile	2.916	2.908	2.910	3.689	3.325	3.110
10^{th} percentile	2.962	2.954	2.954	4.097	3.767	3.611
25^{th} percentile	3.030	3.024	3.022	4.806	4.514	4.475
75^{th} percentile	3.295	3.355	3.334	6.130	5.795	5.780
90^{th} percentile	3.486	3.536	3.526	6.792	6.369	6.391
95^{th} percentile	3.551	3.578	3.569	7.235	6.808	6.819
Std deviation	0.203	0.222	0.219	1.066	1.031	1.083
Variance	0.041	0.049	0.048	1.136	1.064	1.174
Max value	4.434	4.128	4.224	9.880	9.358	9.260
Min value	2.754	2.756	2.754	2.488	2.289	2.277
Fraction OK	0.499	0.603	0.694	0.499	0.603	0.694

Table 3-7. Summary statistics for travel-time and path-length in the tunnels for the crown space, degraded tunnel backfill variant case of the amalgamated repository-scale and regional-scale DFN models. For release time 2020 AD, three paths Q1, Q2, and Q3 were tracked for each of 7,483 release locations in the amalgamated model.

	$Log_{10}(t_t)$ [y]			$Log_{10}(L_t)$ [m]		
	Q1	Q2	Q3	Q1	Q2	Q3
Mean	4.424	3.424	4.505	1.715	1.577	1.671
Median	4.637	4.188	4.501	1.805	1.617	1.738
5th percentile	1.142	–1.150	2.543	0.642	0.446	0.693
10th percentile	2.425	–0.590	2.892	0.848	0.677	0.829
25th percentile	3.624	1.387	3.613	1.263	1.066	1.150
75th percentile	5.530	5.226	5.416	2.207	2.148	2.184
90th percentile	6.184	6.112	6.133	2.423	2.428	2.417
95th percentile	6.531	6.505	6.463	2.544	2.548	2.537
Std deviation	1.570	2.463	1.213	0.607	0.675	0.604
Variance	2.464	6.068	1.472	0.369	0.456	0.364
Max value	8.265	8.217	8.448	3.643	3.478	3.570
Min value	–2.181	–3.191	1.111	–0.621	–1.069	0.225
Fraction OK	0.397	0.603	0.694	0.397	0.603	0.694

Table 3-8. Summary statistics for travel-time and path-length in the EDZ for the crown space, degraded tunnel backfill variant case of the amalgamated repository-scale and regional-scale DFN models. For release time 2020 AD, three paths Q1, Q2, and Q3 were tracked for each of 7,483 release locations in the amalgamated model.

	$Log_{10}(t_{EDZ})$ [y]			$Log_{10}(L_{EDZ})$ [m]		
	Q1	Q2	Q3	Q1	Q2	Q3
Mean	–1.818	–0.880	–1.427	1.697	1.596	1.087
Median	–1.946	–0.944	–1.551	1.782	1.725	1.534
5th percentile	–2.378	–2.763	–2.901	1.255	0.305	–0.847
10th percentile	–2.373	–2.338	–2.397	1.278	0.680	–0.847
25th percentile	–2.336	–1.553	–2.393	1.480	1.314	0.357
75th percentile	–1.158	–0.177	–0.745	1.824	2.025	1.802
90th percentile	–1.144	0.373	–0.092	2.037	2.266	2.226
95th percentile	–1.143	1.613	0.374	2.060	2.384	2.287
Std deviation	0.556	1.189	1.119	0.286	0.620	1.057
Variance	0.309	1.414	1.251	0.082	0.385	1.117
Max value	–1.143	3.118	2.970	2.060	3.012	3.061
Min value	–2.378	–3.928	–4.672	1.255	–0.172	–0.847
Fraction OK	0.001	0.145	0.119	0.001	0.145	0.119

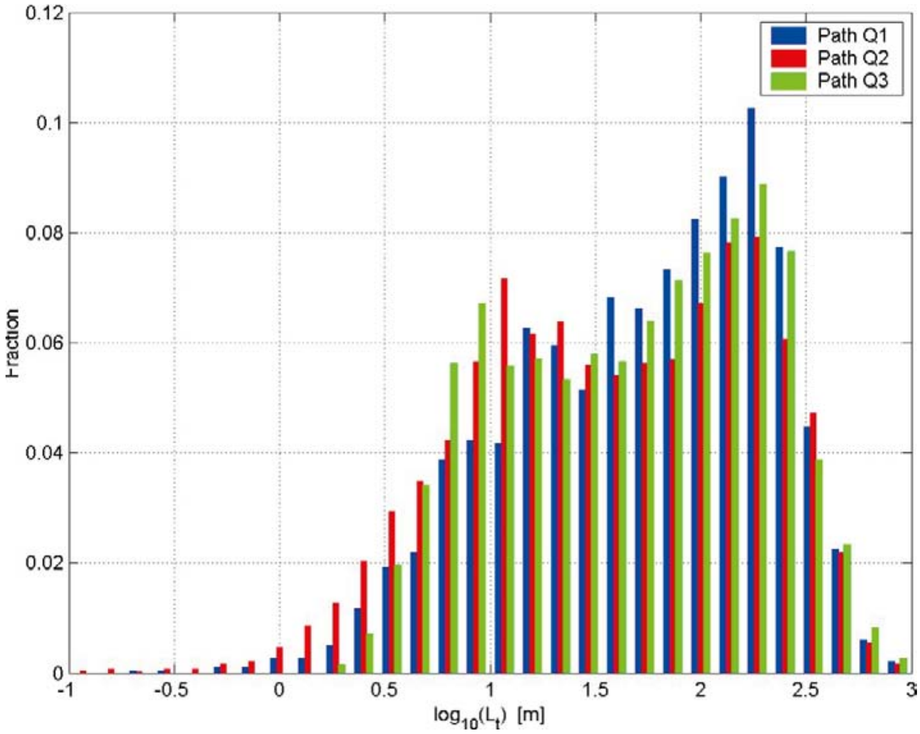

Figure 3-9. *Histograms of path-length in the tunnel, L_t, for paths Q1, Q2 and Q3 in the crown space, degraded tunnel backfill variant of the amalgamated repository-scale and regional-scale DFN models with 7,483 particles released at time 2020 AD.*

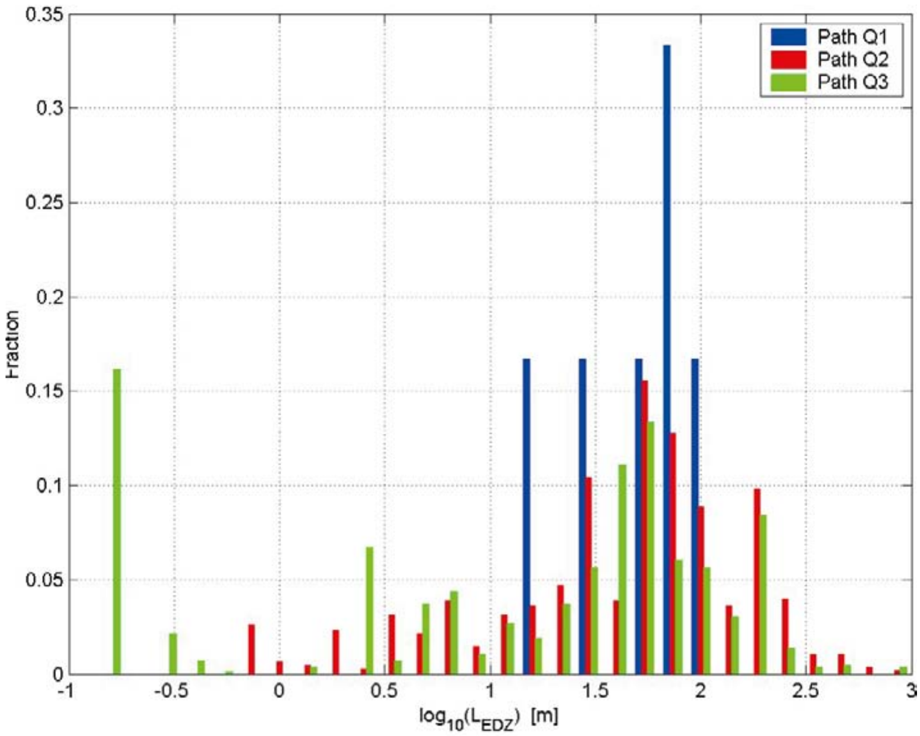

Figure 3-10. *Histograms of path-length in the EDZ, L_{EDZ}, for paths Q1, Q2 and Q3 in the crown space, degraded tunnel backfill variant of the amalgamated repository-scale and regional-scale DFN models with 7,483 particles released at time 2020 AD.*

3.3 Laxemar crown space variant with less transmissive EDZ

This variant model takes the crown space case from Section 3.1 and reduces the transmissivity of the deposition tunnel EDZ from 10^{-8} m^2/s to 10^{-10} m^2/s.

Table 3-9 to Table 3-12 show the performance measure statistics in the rock, the tunnels and the EDZ for this variant case. Comparison to Table 3-1 to Table 3-4 for the crown space base case shows that there is a minor increase in travel time, a decrease in initial Darcy flux and an increase in the flow-related transport resistance for the rock. There is also a minor reduction in the path lengths in the tunnels. There is an increase in the mean time spent in the EDZ for the variant model paths and a decrease in the mean length. The histogram in Figure 3-11 shows a similar distribution of path lengths in the tunnels for this variant compared to the crown space base case shown in Figure 3-6. The histogram in Figure 3-12 shows a reduction in the proportion of longer path lengths in the EDZ for this variant compared to the crown space base case shown in Figure 3-7.

Table 3-9. Summary statistics for travel-time in the rock and for initial Darcy flux for the crown space, less transmissive EDZ variant case of the amalgamated repository-scale and regional-scale DFN models. For release time 2020 AD, three paths Q1, Q2, and Q3 were tracked for each of 7,483 release locations in the amalgamated model.

	$\text{Log}_{10}(t_r)$ [y]			$\text{Log}_{10}(U)$ [m/y]		
	Q1	Q2	Q3	Q1	Q2	Q3
Mean	1.766	1.672	1.677	–3.777	–5.126	–4.260
Median	1.752	1.712	1.695	–3.743	–5.098	–4.424
5th percentile	0.681	0.643	0.618	–6.235	–6.356	–6.741
10th percentile	0.858	0.786	0.757	–5.681	–6.110	–6.281
25th percentile	1.313	1.164	1.164	–4.767	–5.653	–5.448
75th percentile	2.199	2.127	2.141	–2.826	–4.605	–3.218
90th percentile	2.594	2.474	2.495	–1.985	–4.178	–1.921
95th percentile	2.874	2.743	2.769	–1.450	–3.961	–1.199
Std deviation	0.670	0.663	0.681	1.461	0.743	1.666
Variance	0.449	0.440	0.464	2.136	0.553	2.774
Max value	5.887	6.208	5.640	0.717	–2.767	1.163
Min value	–0.091	–0.151	–0.061	–8.321	–7.873	–9.582
Fraction OK	0.478	0.523	0.617	0.686	0.854	1.000

Table 3-10. Summary statistics for path-length and flow-related transport resistance in the rock for the crown space, less transmissive EDZ variant case of the amalgamated repository-scale and regional-scale DFN models. For release time 2020 AD, three paths Q1, Q2, and Q3 were tracked for each of 7,483 release locations in the amalgamated model.

	$\text{Log}_{10}(L_r)$ [m]			$\text{Log}_{10}(F_r)$ [y/m]		
	Q1	Q2	Q3	Q1	Q2	Q3
Mean	3.171	3.177	3.176	5.591	5.394	5.346
Median	3.111	3.109	3.109	5.595	5.431	5.407
5th percentile	2.918	2.908	2.912	3.716	3.549	3.366
10th percentile	2.963	2.954	2.960	4.179	4.116	3.904
25th percentile	3.033	3.026	3.029	4.916	4.821	4.729
75th percentile	3.304	3.300	3.287	6.284	5.994	6.004
90th percentile	3.484	3.527	3.522	6.961	6.549	6.590
95th percentile	3.547	3.580	3.572	7.340	6.990	7.024
Std deviation	0.199	0.219	0.217	1.083	1.002	1.068
Variance	0.039	0.048	0.047	1.173	1.003	1.140
Max value	4.105	4.335	4.683	10.317	10.097	9.831
Min value	2.793	2.758	2.755	2.209	2.204	2.249
Fraction OK	0.478	0.523	0.617	0.478	0.523	0.617

Table 3-11. Summary statistics for travel-time and path-length in the tunnels for the crown space, less transmissive EDZ variant case of the amalgamated repository-scale and regional-scale DFN models. For release time 2020 AD, three paths Q1, Q2, and Q3 were tracked for each of 7,483 release locations in the amalgamated model.

	$Log_{10}(t_t)$ [y]			$Log_{10}(L_t)$ [m]		
	Q1	Q2	Q3	Q1	Q2	Q3
Mean	4.672	4.056	5.274	1.581	1.492	1.608
Median	4.961	4.292	5.262	1.639	1.423	1.575
5th percentile	1.710	0.634	3.874	0.489	0.488	0.726
10th percentile	2.683	1.411	4.153	0.702	0.706	0.844
25th percentile	3.952	3.012	4.670	1.074	1.001	1.073
75th percentile	5.717	5.395	5.866	2.143	2.052	2.140
90th percentile	6.264	6.082	6.355	2.376	2.383	2.405
95th percentile	6.575	6.470	6.655	2.486	2.502	2.519
Std deviation	1.527	1.776	0.865	0.657	0.651	0.604
Variance	2.331	3.154	0.749	0.431	0.423	0.365
Max value	8.161	9.927	9.966	3.032	3.181	3.408
Min value	–2.483	–1.658	2.678	–0.926	–1.455	0.237
Fraction OK	0.368	0.523	0.617	0.368	0.523	0.617

Table 3-12. Summary statistics for travel-time and path-length in the EDZ for the crown space, less transmissive EDZ variant case of the amalgamated repository-scale and regional-scale DFN models. For release time 2020 AD, three paths Q1, Q2, and Q3 were tracked for each of 7,483 release locations in the amalgamated model.

	$Log_{10}(t_{EDZ})$ [y]			$Log_{10}(L_{EDZ})$ [m]		
	Q1	Q2	Q3	Q1	Q2	Q3
Mean	–0.822	0.377	0.154	1.043	1.317	1.280
Median	–0.819	0.355	0.024	1.136	1.401	1.450
5th percentile	–1.525	–1.330	–1.901	0.671	0.271	0.311
10th percentile	–1.525	–0.806	–1.204	0.671	0.576	0.413
25th percentile	–1.348	–0.328	–0.539	0.787	1.012	0.856
75th percentile	–0.297	0.905	0.704	1.277	1.731	1.713
90th percentile	–0.123	1.887	1.887	1.324	1.891	1.802
95th percentile	–0.123	2.280	2.203	1.324	1.975	1.894
Std deviation	0.701	1.187	1.248	0.336	0.516	0.562
Variance	0.491	1.410	1.558	0.113	0.266	0.316
Max value	–0.123	4.910	5.043	1.324	2.990	2.542
Min value	–1.525	–3.484	–3.683	0.671	–0.108	–0.312
Fraction OK	0.000	0.117	0.073	0.000	0.117	0.073

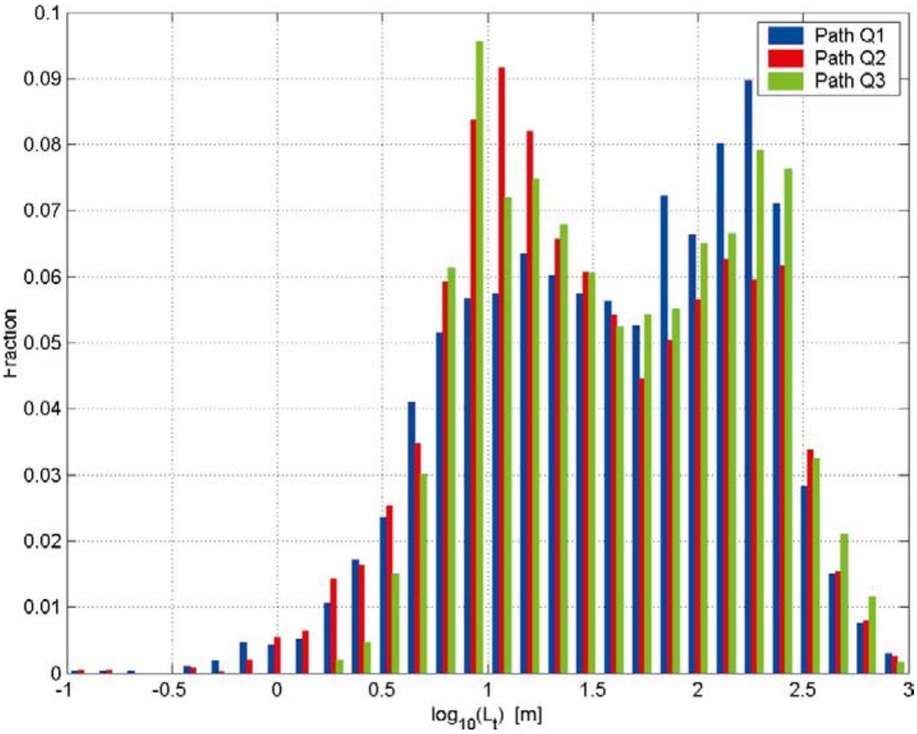

Figure 3-11. Histograms of path-length in the tunnel, L_t, for paths Q1, Q2 and Q3 in the crown space, less transmissive EDZ variant of the amalgamated repository-scale and regional-scale DFN models with 7,483 particles released at time 2020 AD.

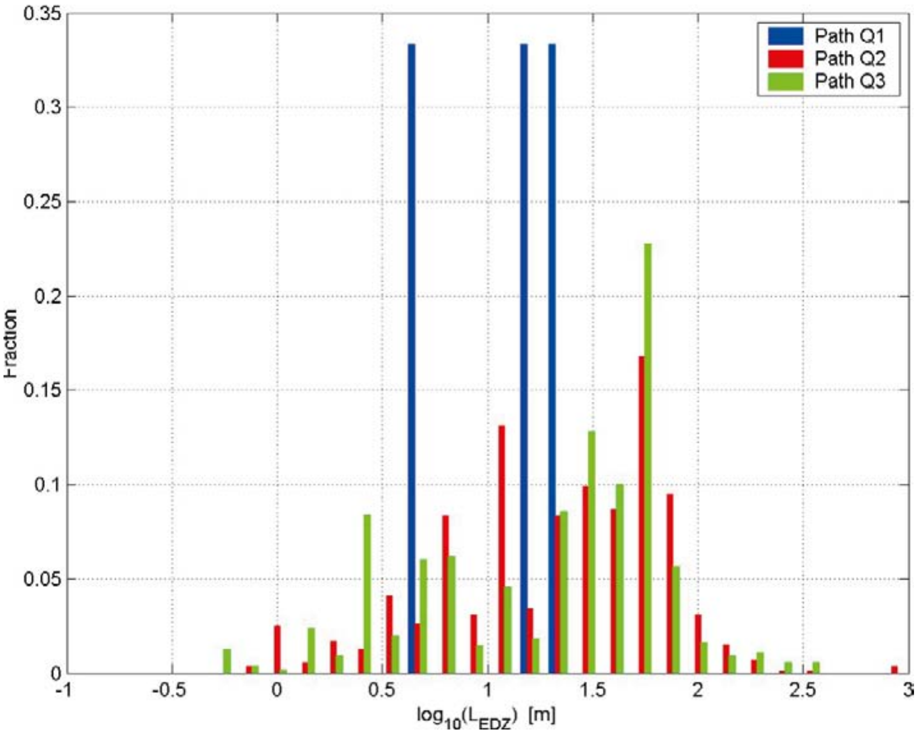

Figure 3-12. Histograms of path-length in the EDZ, L_{EDZ}, for paths Q1, Q2 and Q3 in the crown space, less transmissive EDZ variant of the amalgamated repository-scale and regional-scale DFN models with 7,483 particles released at time 2020 AD

4 Sensitivity analysis of deposition hole EDZ and spalling

4.1 Laxemar deposition hole EDZ variant

This variant model takes the base case from Section 2.2 and adds an EDZ around each deposition hole. This was represented by adding deterministic vertical fractures around each deposition hole, parallel to each face of the hole, with the properties specified in Table 4-1. Two additional cross fractures were added for each deposition hole with the same properties to provide connectivity between the deposition hole and its EDZ. The EDZ fractures were 0.2 m from the deposition hole faces. The cross fractures extended 0.1 m beyond the EDZ fractures. Both the EDZ and the cross fractures extended from the bottom of the deposition hole to the deposition tunnel EDZ. These features are shown in Figure 4-1.

Figure 4-2 shows the release points in the repository in blue and the exit locations at the regional model boundary in red for the deposition hole EDZ variant. Comparison to Figure 2-3 for the base case shows little change in the exit locations for this variant.

Table 4-1. Deposition hole EDZ properties.

Parameter	Value
Deposition hole EDZ transmissivity	10^{-9} m^2/s
Deposition hole EDZ porosity	10^{-5}
Deposition hole EDZ thickness	0.1 m

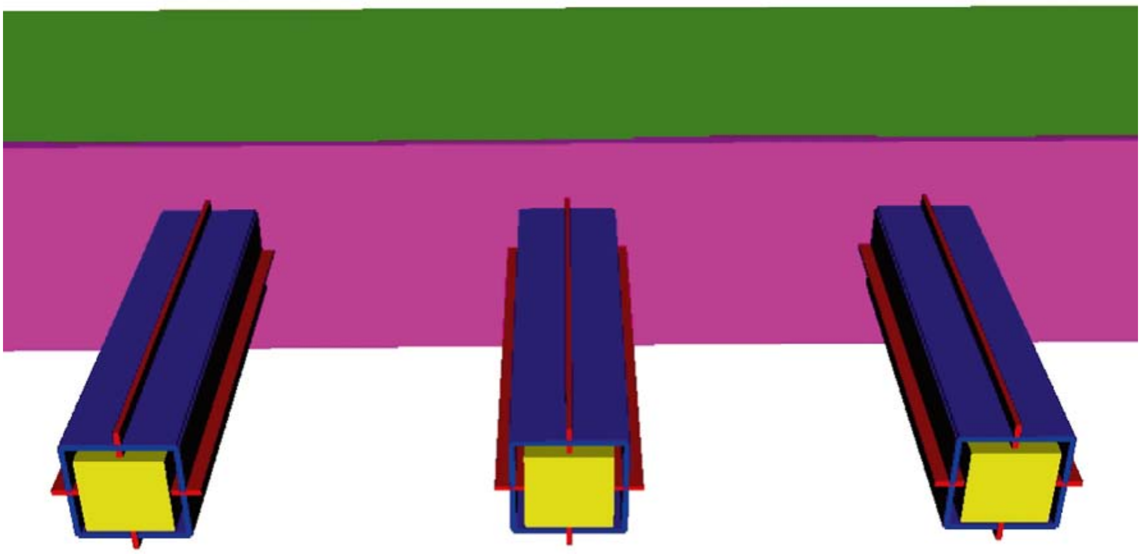

Figure 4-1. *Deposition hole EDZ viewed from below. Deposition tunnels are coloured green, the deposition tunnel EDZ is coloured purple, deposition holes are coloured yellow, the deposition hole EDZ is coloured blue and the cross fractures are coloured red.*

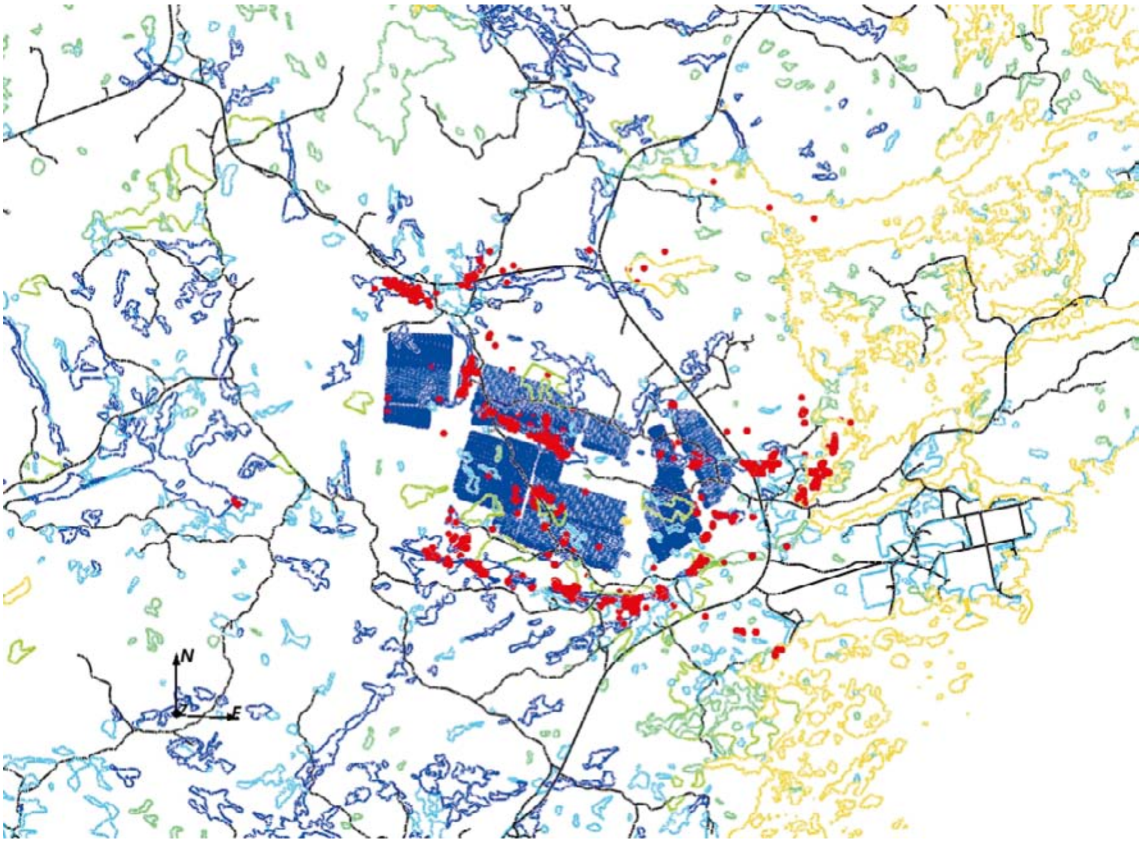

Figure 4-2. *Particle release and exit points viewed from above, for paths Q1, Q2 and Q3 in the deposition hole EDZ variant of the amalgamated repository-scale and regional-scale DFN models with 7,483 particles released at time 2020 AD. Release points are coloured blue and exit locations are coloured red.*

For this case, the Q1 release points include the deposition hole EDZ and cross fractures, as well as the existing fractures. Therefore, there are additional paths available for the Q1 particles to follow.

Table 4-2 to Table 4-5 show the performance measure statistics in the rock, the tunnels and the tunnel EDZ for this case. Particles in the deposition hole EDZ are taken to be in the rock. Comparison to Table 2-3 to Table 2-6 for the base case shows that there is a minor reduction in mean travel times in the rock. There is also a minor increase in mean path lengths in the rock for the Q1 paths, but a minor decrease for the Q2 and Q3 paths. The mean initial Darcy flux shows a minor increase for this case. There is also a minor increase in the mean travel times and mean path lengths in the tunnels. There is a reduction in the mean time spent in the tunnel EDZ for this case, especially for the Q2 and Q3 paths and a minor decrease in the mean length in the tunnel EDZ. The cumulative distribution function plots in Figure 4-3, Figure 4-5 and Figure 4-6 show a decrease in the proportion of paths with higher values for travel time, path length and flow-related transport resistance respectively in the rock compared to the corresponding plots for the base case in Figure 2-4, Figure 2-6 and Figure 2-7. The cumulative distribution function plot in Figure 4-4 shows little difference in the distribution of initial Darcy velocities in the rock compared to the corresponding base case plot in Figure 2-5. The histogram in Figure 4-7 shows a greater proportion of paths with both shorter and longer lengths in the tunnels for the Q1 paths, but little difference for Q2 and Q3 for this case compared to the base case shown in Figure 2-8. The histogram in Figure 4-8 shows a lower proportion of paths with longer lengths in the tunnel EDZ for the Q2 and Q3 paths, but little change for Q1 for this variant compared to the base case shown in Figure 2-9.

These results suggest that there was flow along the deposition hole EDZ towards the deposition tunnels. This gave an increase in the travel time and path lengths in the tunnels. However, for the Q2 and Q3 particles this flow moved particles away from the tunnel EDZ, giving a reduction in travel times and path lengths in the tunnel EDZ. Figure 4-9 shows a Q1 particle travelling up the deposition hole EDZ to a deposition tunnel.

The fraction of Q1 particles reaching the boundary was much higher for this variant than for the base case due to the greater availability of starting locations provided by the deposition hole EDZ fractures. The deposition hole EDZ fractures had flow because there were flow pathways available both from rock fractures and also from the tunnel EDZ. The fraction of Q2 paths reaching the boundary was slightly reduced because there was flow available from the tunnel EDZ to the deposition hole EDZ and then out through a rock fracture. Thus the deposition hole EDZ added different types of connections and flow patterns around the deposition holes.

Table 4-2. Summary statistics for travel-time in the rock and for initial Darcy flux for the deposition hole EDZ variant of the amalgamated repository-scale and regional-scale DFN models. For release time 2020 AD, three paths Q1, Q2, and Q3 were tracked for each of 7,483 release locations in the amalgamated model.

	$Log_{10}(t_r)$ [y]			$Log_{10}(U)$ [m/y]		
	Q1	Q2	Q3	Q1	Q2	Q3
Mean	1.694	1.632	1.681	–3.585	–3.196	–4.002
Median	1.706	1.637	1.688	–3.664	–3.187	–4.050
5th percentile	0.745	0.670	0.702	–5.045	–3.985	–5.656
10th percentile	0.913	0.826	0.858	–4.777	–3.785	–5.298
25th percentile	1.305	1.177	1.233	–4.285	–3.499	–4.746
75th percentile	2.092	2.101	2.129	–3.008	–2.878	–3.397
90th percentile	2.399	2.398	2.456	–2.399	–2.616	–2.713
95th percentile	2.597	2.606	2.648	–1.877	–2.469	–2.027
Std deviation	0.567	0.598	0.603	1.001	0.468	1.122
Variance	0.322	0.358	0.363	1.002	0.219	1.258
Max value	4.816	3.312	4.305	2.105	–0.730	0.667
Min value	–0.105	–0.191	–0.040	–5.793	–4.796	–8.821
Fraction OK	0.855	0.598	0.673	0.999	0.886	1.000

Table 4-3. Summary statistics for path-length and flow-related transport resistance in the rock for the deposition hole EDZ variant of the amalgamated repository-scale and regional-scale DFN models. For release time 2020 AD, three paths Q1, Q2, and Q3 were tracked for each of 7,483 release locations in the amalgamated model.

	$Log_{10}(L_r)$ [m]			$Log_{10}(F_r)$ [y/m]		
	Q1	Q2	Q3	Q1	Q2	Q3
Mean	3.196	3.153	3.162	5.680	5.463	5.584
Median	3.147	3.110	3.117	5.753	5.564	5.665
5th percentile	2.935	2.920	2.914	4.287	3.768	3.939
10th percentile	2.982	2.964	2.962	4.721	4.329	4.497
25th percentile	3.058	3.033	3.040	5.262	5.038	5.170
75th percentile	3.317	3.223	3.248	6.165	6.000	6.105
90th percentile	3.500	3.471	3.468	6.554	6.415	6.552
95th percentile	3.558	3.533	3.532	6.816	6.684	6.832
Std deviation	0.197	0.183	0.186	0.783	0.857	0.866
Variance	0.039	0.034	0.035	0.612	0.735	0.749
Max value	4.260	4.198	4.266	9.058	8.663	9.224
Min value	2.784	2.758	2.767	2.267	2.302	2.497
Fraction OK	0.855	0.598	0.673	0.855	0.598	0.673

Table 4-4. Summary statistics for travel-time and path-length in the tunnels for the deposition hole EDZ variant of the amalgamated repository-scale and regional-scale DFN models. For release time 2020 AD, three paths Q1, Q2, and Q3 were tracked for each of 7,483 release locations in the amalgamated model.

	$Log_{10}(t_t)$ [y]			$Log_{10}(L_t)$ [m]		
	Q1	Q2	Q3	Q1	Q2	Q3
Mean	5.228	5.084	5.592	1.227	1.121	1.299
Median	5.392	5.235	5.577	1.232	1.134	1.265
5th percentile	3.239	3.139	4.455	0.347	0.198	0.706
10th percentile	3.718	3.551	4.660	0.591	0.467	0.826
25th percentile	4.620	4.317	5.083	0.892	0.781	1.000
75th percentile	5.991	5.918	6.079	1.572	1.475	1.571
90th percentile	6.415	6.364	6.553	1.854	1.764	1.840
95th percentile	6.655	6.608	6.817	2.061	1.949	1.988
Std deviation	1.038	1.086	0.716	0.532	0.523	0.408
Variance	1.077	1.180	0.513	0.283	0.274	0.167
Max value	7.765	8.575	8.935	2.905	2.787	2.840
Min value	–0.421	1.298	3.468	–1.021	–0.848	0.152
Fraction OK	0.701	0.501	0.673	0.701	0.501	0.673

Table 4-5. Summary statistics for travel-time and path-length in the tunnel EDZ for the deposition hole EDZ variant of the amalgamated repository-scale and regional-scale DFN models. For release time 2020 AD, three paths Q1, Q2, and Q3 were tracked for each of 7,483 release locations in the amalgamated model.

	$Log_{10}(t_{EDZ})$ [y]			$Log_{10}(L_{EDZ})$ [m]		
	Q1	Q2	Q3	Q1	Q2	Q3
Mean	–0.375	–0.547	–0.348	1.239	1.137	1.267
Median	–0.340	–0.479	–0.298	1.308	1.202	1.344
5th percentile	–1.687	–2.120	–1.884	0.159	0.003	0.200
10th percentile	–1.340	–1.666	–1.395	0.552	0.189	0.529
25th percentile	–0.831	–1.015	–0.824	0.905	0.815	0.888
75th percentile	0.136	–0.004	0.170	1.607	1.570	1.673
90th percentile	0.538	0.411	0.585	1.872	1.860	1.914
95th percentile	0.740	0.673	0.937	2.022	1.997	2.036
Std deviation	0.752	0.854	0.876	0.544	0.606	0.555
Variance	0.565	0.729	0.768	0.296	0.367	0.308
Max value	2.407	3.176	3.953	2.440	2.798	2.913
Min value	–3.409	–4.460	–5.269	–1.115	–1.028	–0.922
Fraction OK	0.531	0.598	0.349	0.531	0.598	0.349

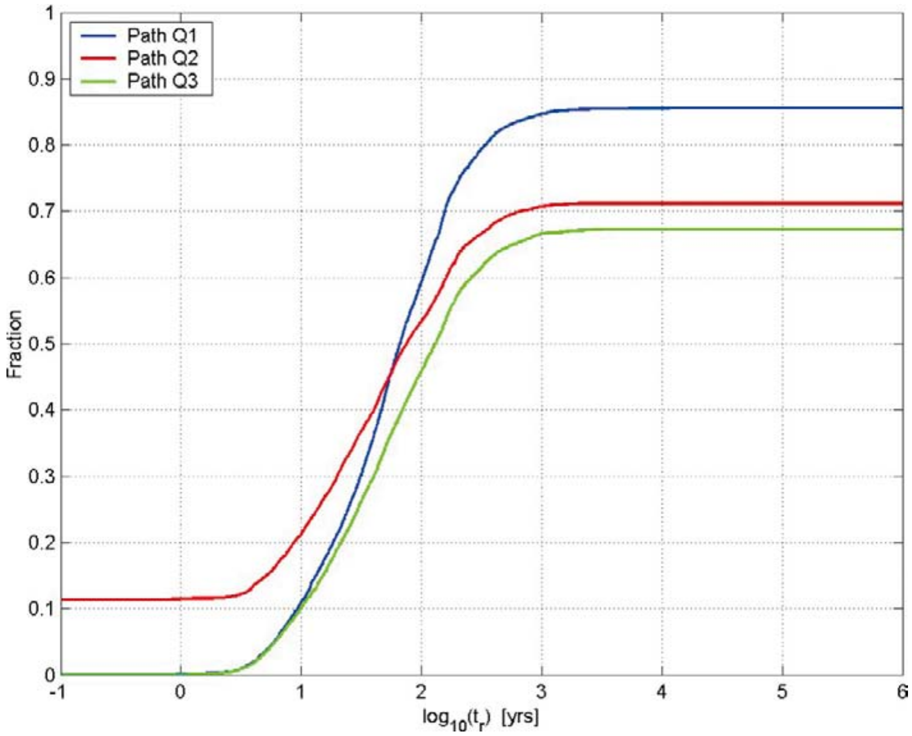

Figure 4-3. *Cumulative distribution plots of travel-time in the rock, t_r, for paths Q1, Q2 and Q3 in the deposition hole EDZ variant of the amalgamated repository-scale and regional-scale DFN models with 7,483 particles released at time 2020 AD.*

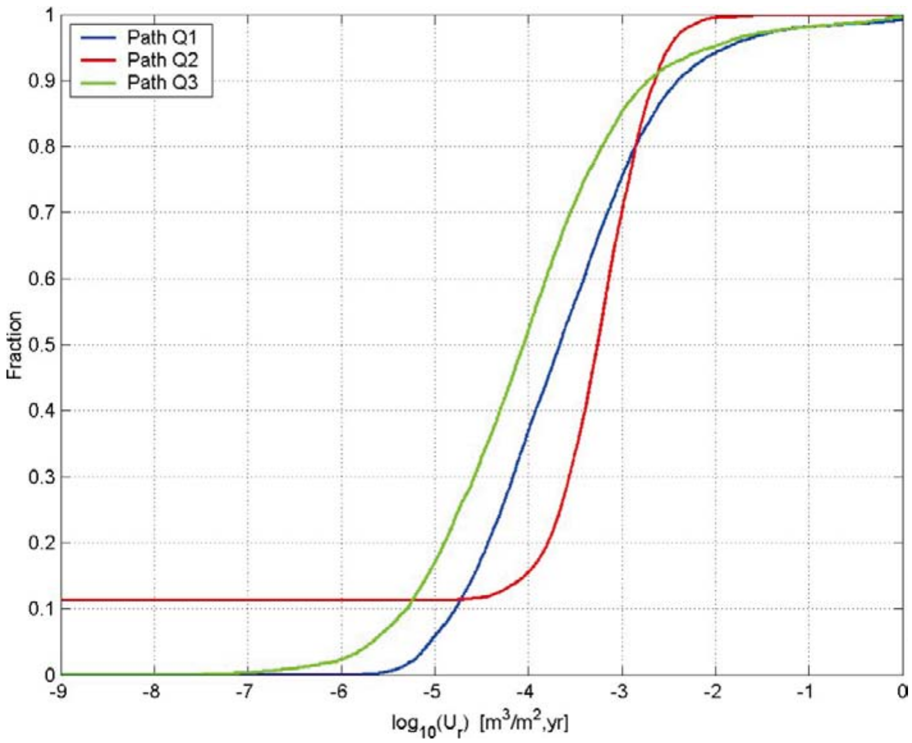

Figure 4-4. *Cumulative distribution plots of initial Darcy flux, U, for paths Q1, Q2 and Q3 in the deposition hole EDZ variant of the amalgamated repository-scale and regional-scale DFN models with 7,483 particles released at time 2020 AD.*

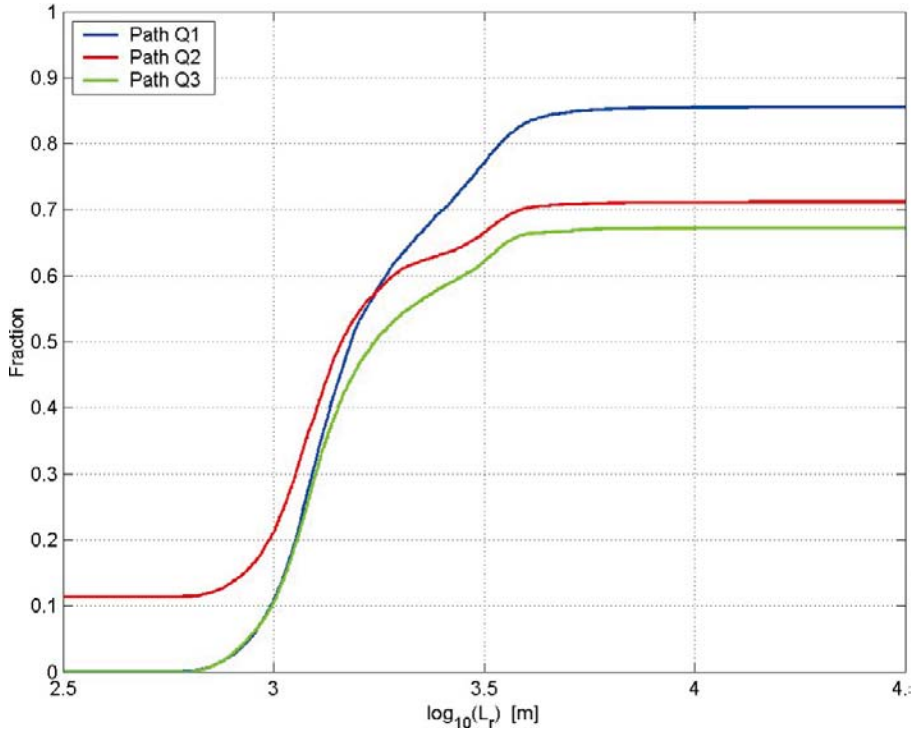

Figure 4-5. *Cumulative distribution plot of path-length in the rock, L_r, for paths Q1, Q2 and Q3 in deposition hole EDZ variant of the amalgamated repository-scale and regional-scale DFN models with 7,483 particles released at time 2020 AD.*

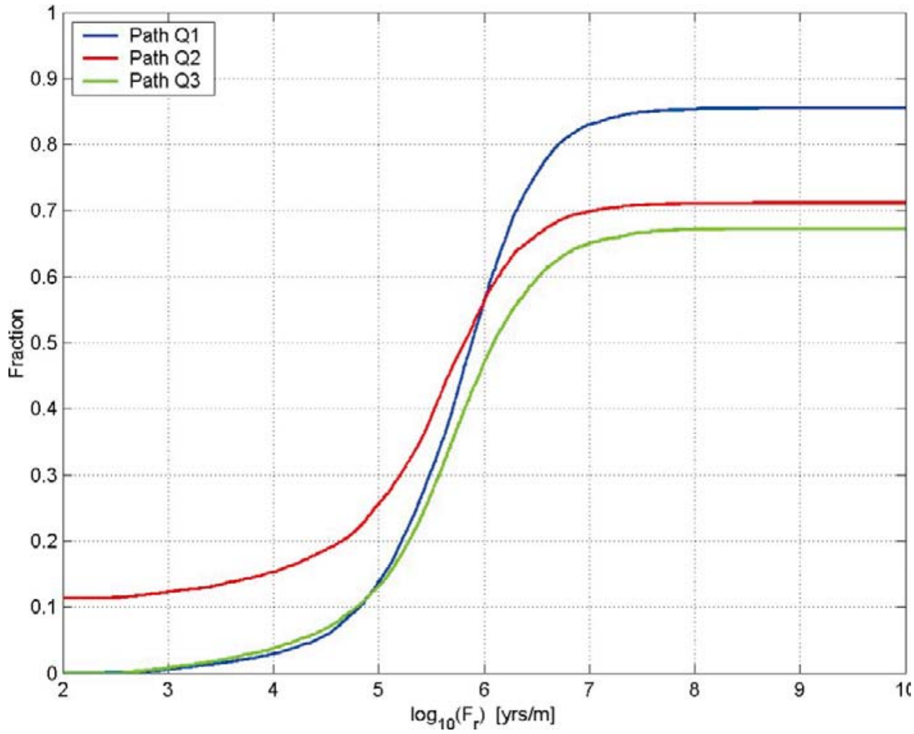

Figure 4-6. *Cumulative distribution plots of flow-related transport resistance in the rock, F_r, for paths Q1, Q2 and Q3 in the deposition hole EDZ variant of the amalgamated repository-scale and regional-scale DFN models with 7,483 particles released at time 2020 AD.*

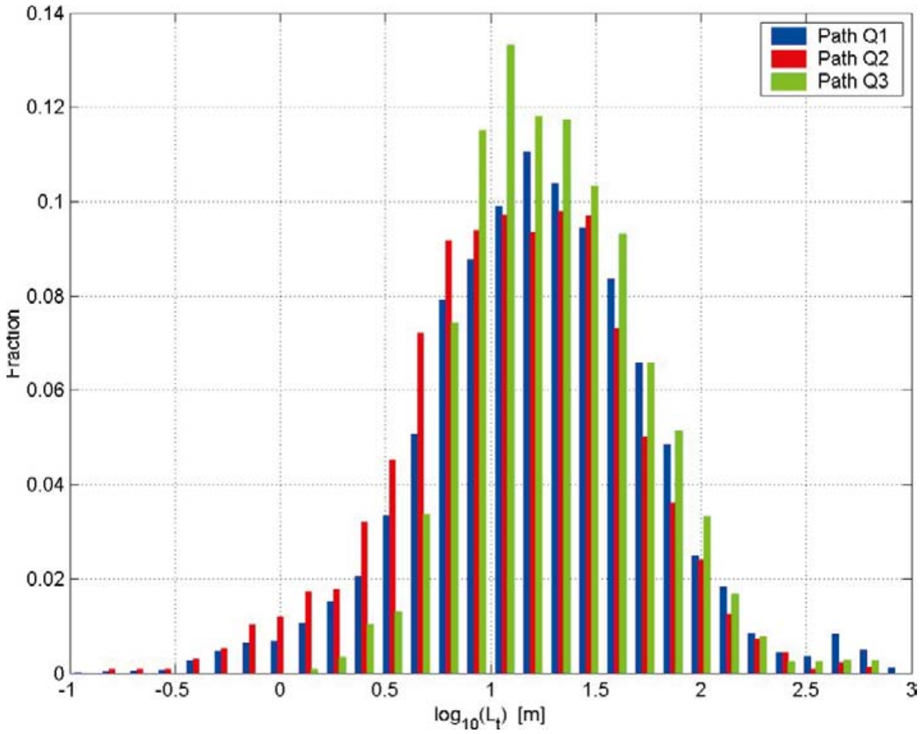

Figure 4-7. *Histograms of path-length in the tunnel, L_t, for paths Q1, Q2 and Q3 in the deposition hole EDZ variant of the amalgamated repository-scale and regional-scale DFN models with 7,483 particles released at time 2020 AD.*

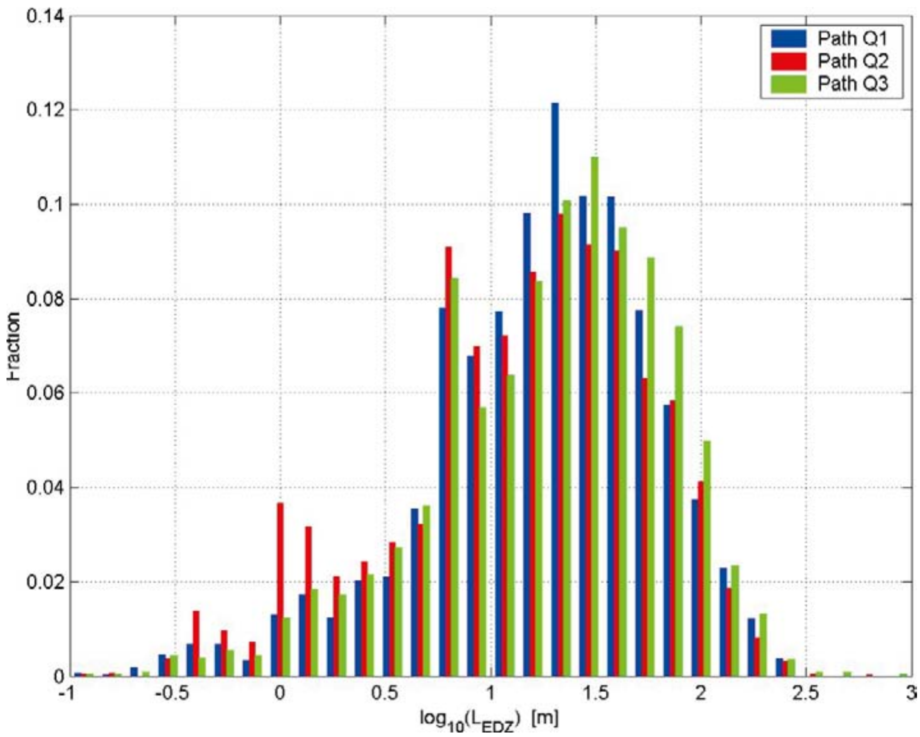

Figure 4-8. *Histograms of path-length in the tunnel EDZ, L_{EDZ}, for paths Q1, Q2 and Q3 in the deposition hole EDZ variant of the amalgamated repository-scale and regional-scale DFN models with 7,483 particles released at time 2020 AD.*

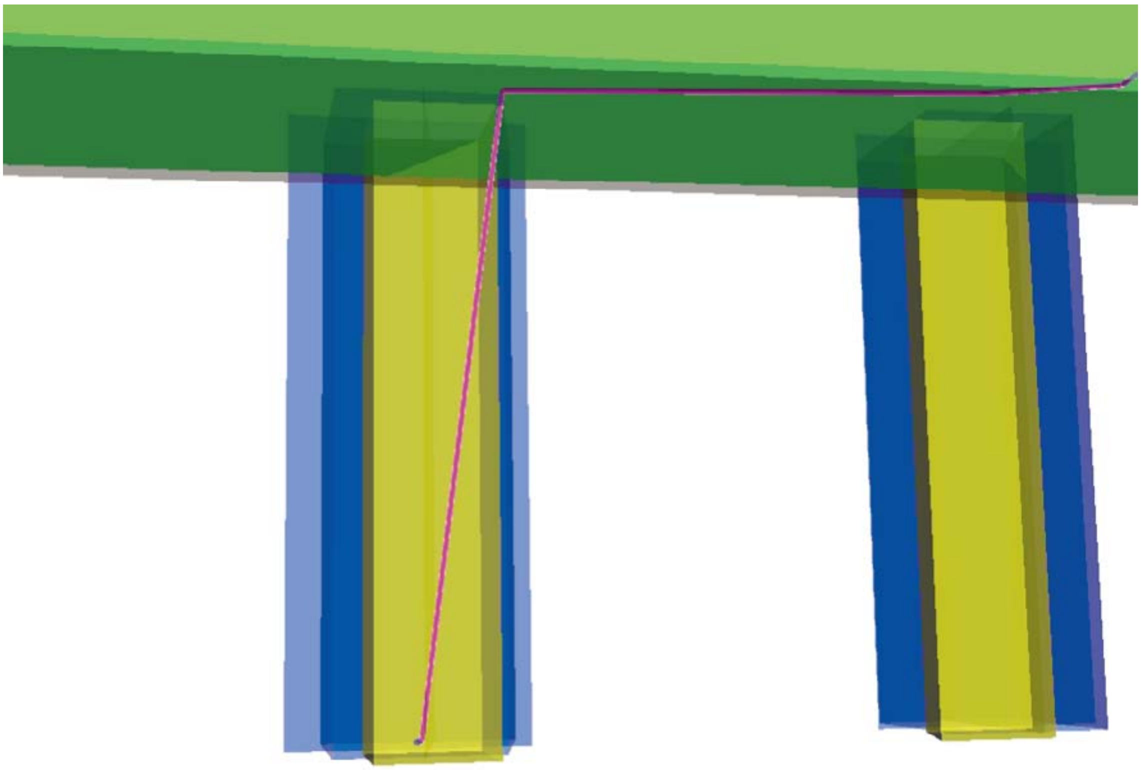

***Figure 4-9.** A particle path from a Q1 release point travelling up the deposition hole EDZ to the deposition tunnel. The deposition tunnel is coloured green, the deposition hole EDZ is coloured blue, the deposition hole is coloured yellow, the particle start point is coloured blue and the particle path is coloured purple. Transparency has been applied and fractures removed to make the path visible. Other paths have been removed.*

4.2 Laxemar deposition hole EDZ and spalling variant

This variant model takes the deposition hole EDZ variant from Section 4.1 and represents spalling by changing the properties of the cross fractures as shown in *Table 4-6*. The porosity of the spalling was uncertain and so the same value was used as for the tunnels. The properties of the deposition hole EDZ fractures remained as shown in Table 4-1.

Table 4-7 to Table 4-10 show the performance measure statistics in the rock, the tunnels and the tunnel EDZ for this variant case. Comparison to Table 4-2 to Table 4-5 for the deposition hole EDZ variant shows that there is an increase in mean travel time and mean initial Darcy flux, particularly with Q1 particles for the latter. There are also minor increases in mean travel time and mean path length in the tunnels. There is a reduction in the mean travel time and mean path length in the tunnel EDZ. The cumulative distribution function plot in Figure 4-10 shows a higher proportion of paths with longer travel times in the rock compared to the plot in Figure 4-3. The histogram in Figure 4-11 shows a similar distribution of path lengths in the tunnels for this variant compared to the deposition hole EDZ variant shown in Figure 4-7. The histogram in Figure 4-12 also shows a similar distribution of path lengths in the tunnel EDZ for this variant compared to the deposition hole EDZ variant shown in Figure 4-8.

The increase in mean travel times in the rock in this variant compared to the deposition hole EDZ variant was due to time spent in the deposition hole spalling, which had a high porosity. Even though the initial Darcy flux was higher here due to the increased hydraulic conductivity of the spalling, there was a reduction in transport velocity due to the higher porosity of the spalling.

Table 4-6. Deposition hole EDZ properties.

Parameter	Value
Deposition hole spalling transmissivity	10^{-5} m^2/s
Deposition hole spalling porosity	0.35
Deposition hole spalling thickness	0.1 m

Table 4-7. Summary statistics for travel-time in the rock and for initial Darcy flux for the deposition hole spalling variant case of the amalgamated repository-scale and regional-scale DFN models. For release time 2020 AD, three paths Q1, Q2, and Q3 were tracked for each of 7,483 release locations in the amalgamated model.

	$Log_{10}(t_r)$ [y]			$Log_{10}(U)$ [m/y]		
	Q1	Q2	Q3	Q1	Q2	Q3
Mean	2.606	2.288	2.252	–2.991	–3.175	–3.786
Median	2.637	2.308	2.255	–3.046	–3.161	–3.820
5th percentile	1.254	0.800	0.818	–4.313	–3.979	–5.340
10th percentile	1.629	1.076	1.038	–4.049	–3.780	–4.970
25th percentile	2.147	1.684	1.612	–3.579	–3.480	–4.413
75th percentile	3.114	2.868	2.846	–2.499	–2.859	–3.239
90th percentile	3.527	3.358	3.362	–1.965	–2.601	–2.601
95th percentile	3.774	3.660	3.695	–1.540	–2.448	–2.041
Std deviation	0.758	0.887	0.894	0.889	0.479	1.046
Variance	0.575	0.786	0.800	0.790	0.229	1.094
Max value	6.219	5.675	6.242	2.139	0.160	1.356
Min value	–0.002	–0.107	–0.078	–5.594	–5.196	–8.931
Fraction OK	0.825	0.581	0.660	1.000	0.883	1.000

Table 4-8. Summary statistics for path-length and flow-related transport resistance in the rock for the deposition hole spalling variant case of the amalgamated repository-scale and regional-scale DFN models. For release time 2020 AD, three paths Q1, Q2, and Q3 were tracked for each of 7,483 release locations in the amalgamated model.

	$Log_{10}(L_r)$ [m]			$Log_{10}(F_r)$ [y/m]		
	Q1	Q2	Q3	Q1	Q2	Q3
Mean	3.199	3.168	3.174	5.533	5.469	5.540
Median	3.153	3.120	3.126	5.608	5.557	5.616
5^{th} percentile	2.937	2.923	2.920	4.049	3.847	3.972
10^{th} percentile	2.986	2.967	2.961	4.511	4.424	4.479
25^{th} percentile	3.063	3.041	3.039	5.103	5.045	5.127
75^{th} percentile	3.321	3.249	3.280	6.033	5.972	6.039
90^{th} percentile	3.499	3.494	3.496	6.438	6.371	6.426
95^{th} percentile	3.560	3.544	3.551	6.679	6.656	6.753
Std deviation	0.194	0.190	0.195	0.801	0.844	0.834
Variance	0.038	0.036	0.038	0.641	0.712	0.695
Max value	4.193	4.022	4.319	8.843	8.811	8.741
Min value	2.774	2.771	2.762	2.434	2.413	2.402
Fraction OK	0.825	0.581	0.660	0.825	0.581	0.660

Table 4-9. Summary statistics for travel-time and path-length in the tunnels for the deposition hole spalling variant case of the amalgamated repository-scale and regional-scale DFN models. For release time 2020 AD, three paths Q1, Q2, and Q3 were tracked for each of 7,483 release locations in the amalgamated model.

	$Log_{10}(t_t)$ [y]			$Log_{10}(L_t)$ [m]		
	Q1	Q2	Q3	Q1	Q2	Q3
Mean	5.348	5.290	5.660	1.393	1.311	1.418
Median	5.525	5.487	5.659	1.391	1.327	1.385
5th percentile	3.430	3.242	4.476	0.577	0.450	0.772
10th percentile	3.911	3.775	4.705	0.772	0.640	0.874
25th percentile	4.770	4.682	5.137	1.056	0.966	1.089
75th percentile	6.091	6.074	6.192	1.738	1.677	1.718
90th percentile	6.474	6.447	6.592	2.041	1.955	2.009
95th percentile	6.682	6.637	6.823	2.212	2.137	2.187
Std deviation	1.005	1.050	0.727	0.518	0.529	0.445
Variance	1.010	1.102	0.529	0.269	0.280	0.198
Max value	8.501	7.645	8.188	2.935	2.882	3.031
Min value	–0.438	1.229	3.290	–0.729	–0.716	0.236
Fraction OK	0.739	0.512	0.660	0.739	0.512	0.660

Table 4-10. Summary statistics for travel-time and path-length in the tunnel EDZ for the deposition hole spalling variant case of the amalgamated repository-scale and regional-scale DFN models. For release time 2020 AD, three paths Q1, Q2, and Q3 were tracked for each of 7,483 release locations in the amalgamated model.

	$Log_{10}(t_{EDZ})$ [y]			$Log_{10}(L_{EDZ})$ [m]		
	Q1	Q2	Q3	Q1	Q2	Q3
Mean	–0.462	–0.561	–0.436	1.184	1.087	1.188
Median	–0.417	–0.533	–0.396	1.244	1.141	1.268
5th percentile	–1.809	–2.111	–1.958	0.128	0.013	0.152
10th percentile	–1.423	–1.706	–1.541	0.479	0.185	0.418
25th percentile	–0.906	–1.090	–0.935	0.855	0.760	0.838
75th percentile	0.046	–0.056	0.073	1.570	1.526	1.573
90th percentile	0.426	0.397	0.503	1.818	1.810	1.837
95th percentile	0.660	0.720	0.994	1.961	1.950	1.992
Std deviation	0.754	0.911	0.903	0.544	0.608	0.577
Variance	0.569	0.830	0.815	0.296	0.370	0.333
Max value	2.966	2.931	3.067	2.756	3.227	3.226
Min value	–3.489	–4.516	–5.739	–1.056	–1.437	–1.483
Fraction OK	0.452	0.581	0.323	0.452	0.581	0.323

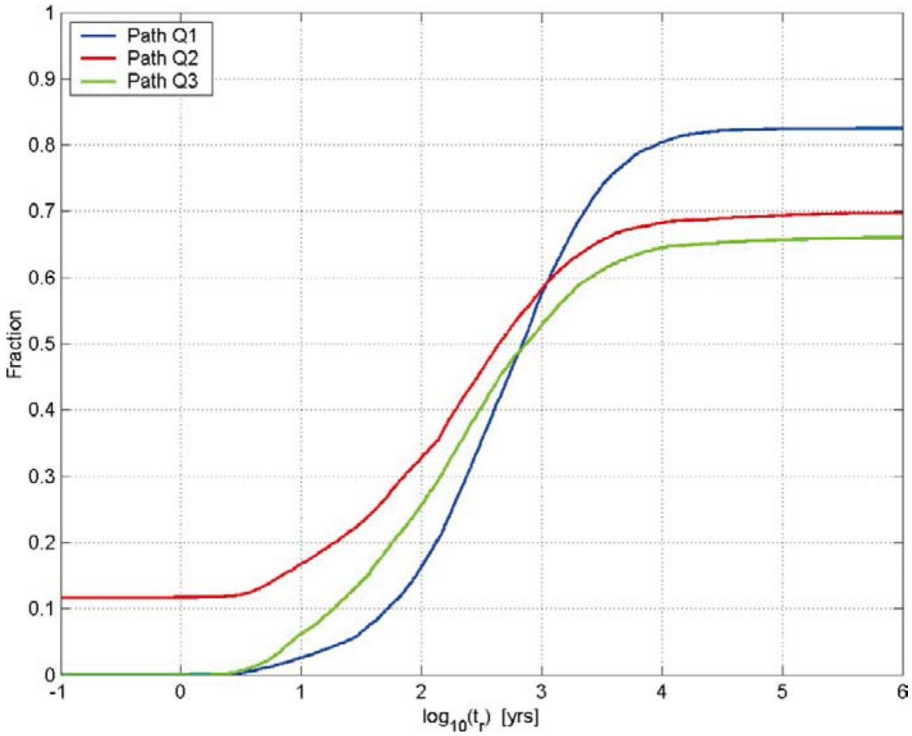

Figure 4-10. Cumulative distribution plots of travel-time in the rock, t_r, for paths Q1, Q2 and Q3 in the deposition hole spalling variant of the amalgamated repository-scale and regional-scale DFN models with 7,483 particles released at time 2020 AD.

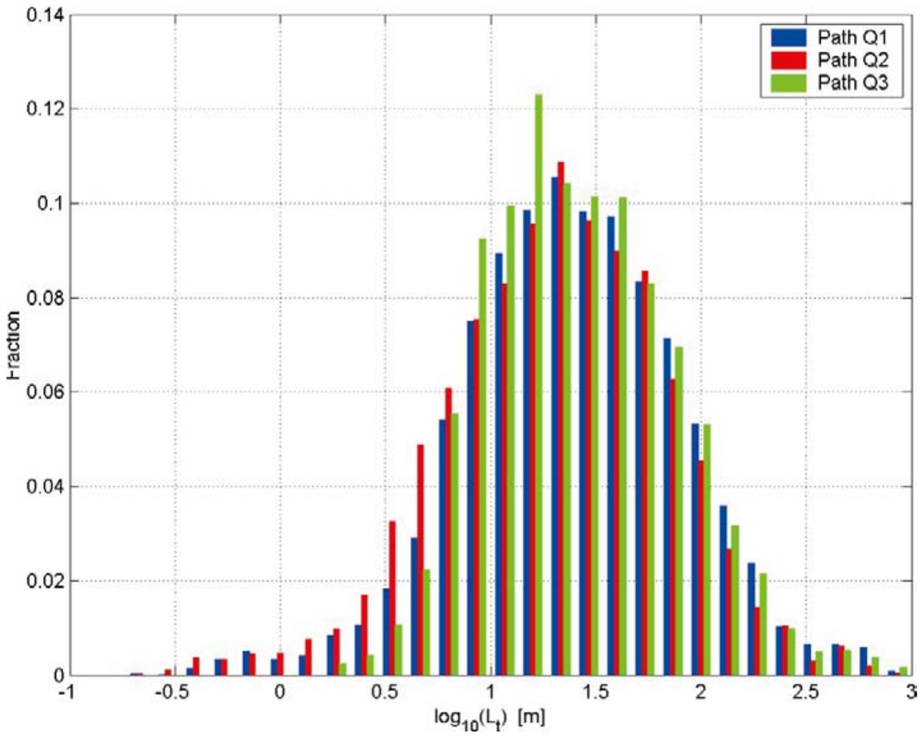

Figure 4-11. Histograms of path-length in the tunnel, L_t, for paths Q1, Q2 and Q3 in the deposition hole spalling variant of the amalgamated repository-scale and regional-scale DFN models with 7,483 particles released at time 2020 AD.

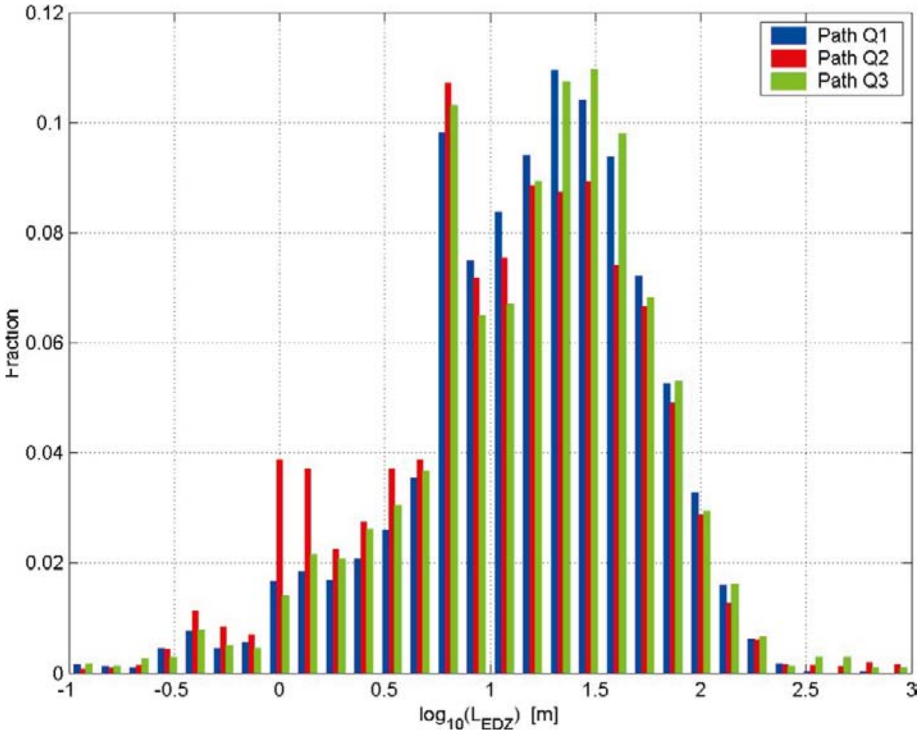

Figure 4-12. Histograms of path-length in the tunnel EDZ, L_{EDZ}, for paths Q1, Q2 and Q3 in the deposition hole spalling variant of the amalgamated repository-scale and regional-scale DFN models with 7,483 particles released at time 2020 AD.

4.3 Laxemar deposition hole EDZ and spalling variant with degraded deposition tunnel EDZ

This variant model takes the deposition hole EDZ and spalling variant from Section 4.2 and increases the transmissivity of the deposition tunnel EDZ from 10^{-8} m^2/s to 10^{-6} m^2/s.

Table 4-11 to Table 4-14 show the performance measure statistics in the rock, the tunnels and the tunnel EDZ for this variant case. Comparison to Table 4-7 to Table 4-10 for the deposition hole EDZ and spalling variant shows that there is a decrease in mean travel time, a slight decrease in mean path length, an increase in mean initial Darcy flux (especially for the Q2 release points) and a decrease in mean flow-related transport resistance for the rock. There is also a minor decrease in the mean path length in the tunnels. There is a decrease in the mean time spent in the tunnel EDZ for the variant model paths and an increase in the mean path length. The histogram in Figure 4-13 shows a similar distribution of path lengths in the tunnels for this variant compared to the deposition hole EDZ and spalling variant shown in Figure 4-11. The histogram in Figure 4-14 shows an increase in the proportion of longer path lengths in the tunnel EDZ for this variant compared to the deposition hole EDZ and spalling variant shown in Figure 4-12.

These results suggest that there was additional flow in to the deposition tunnel EDZ for this variant compared to the deposition hole EDZ and spalling variant and that the velocity in the deposition tunnel EDZ was higher.

Table 4-11. Summary statistics for travel-time in the rock and for initial Darcy flux for the deposition hole spalling, degraded tunnel EDZ variant case of the amalgamated repository-scale and regional-scale DFN models. For release time 2020 AD, three paths Q1, Q2, and Q3 were tracked for each of 7,483 release locations in the amalgamated model.

	$Log_{10}(t_r)$ [y]			$Log_{10}(U)$ [m/y]		
	Q1	Q2	Q3	Q1	Q2	Q3
Mean	2.418	1.893	1.967	–2.707	–1.831	–3.284
Median	2.419	1.907	1.967	–2.699	–1.738	–3.334
5th percentile	1.147	0.629	0.683	–4.220	–3.037	–5.355
10th percentile	1.466	0.787	0.849	–3.918	–2.762	–4.913
25th percentile	1.931	1.255	1.365	–3.346	–2.278	–4.162
75th percentile	2.918	2.448	2.507	–2.148	–1.349	–2.349
90th percentile	3.383	2.951	3.040	–1.570	–1.021	–1.550
95th percentile	3.652	3.261	3.360	–1.195	–0.845	–1.201
Std deviation	0.750	0.815	0.822	0.944	0.685	1.301
Variance	0.562	0.664	0.676	0.891	0.469	1.694
Max value	5.294	4.696	4.647	3.273	1.417	1.911
Min value	0.008	–0.104	–0.129	–5.545	–4.734	–8.273
Fraction OK	0.792	0.581	0.638	0.999	0.950	1.000

Table 4-12. Summary statistics for path-length and flow-related transport resistance in the rock for the deposition hole spalling, degraded tunnel EDZ variant case of the amalgamated repository-scale and regional-scale DFN models. For release time 2020 AD, three paths Q1, Q2, and Q3 were tracked for each of 7,483 release locations in the amalgamated model.

	$Log_{10}(L_r)$ [m]			$Log_{10}(F_r)$ [y/m]		
	Q1	Q2	Q3	Q1	Q2	Q3
Mean	3.168	3.124	3.137	5.236	4.959	5.181
Median	3.118	3.082	3.089	5.299	5.104	5.298
5^{th} percentile	2.929	2.912	2.911	3.714	3.150	3.479
10^{th} percentile	2.974	2.951	2.955	4.106	3.607	3.933
25^{th} percentile	3.040	3.013	3.021	4.746	4.390	4.691
75^{th} percentile	3.274	3.178	3.211	5.776	5.589	5.744
90^{th} percentile	3.466	3.432	3.435	6.229	6.032	6.198
95^{th} percentile	3.533	3.515	3.513	6.503	6.323	6.494
Std deviation	0.187	0.175	0.178	0.844	0.934	0.891
Variance	0.035	0.031	0.032	0.712	0.872	0.794
Max value	4.303	3.940	3.945	9.161	8.293	8.573
Min value	2.776	2.757	2.762	2.322	2.263	2.356
Fraction OK	0.792	0.581	0.638	0.792	0.581	0.638

Table 4-13. Summary statistics for travel-time and path-length in the tunnels for the deposition hole spalling, degraded tunnel EDZ variant case of the amalgamated repository-scale and regional-scale DFN models. For release time 2020 AD, three paths Q1, Q2, and Q3 were tracked for each of 7,483 release locations in the amalgamated model.

	$Log_{10}(t_t)$ [y]			$Log_{10}(L_t)$ [m]		
	Q1	Q2	Q3	Q1	Q2	Q3
Mean	5.261	5.219	5.634	1.315	1.229	1.366
Median	5.395	5.377	5.669	1.337	1.289	1.335
5th percentile	3.376	3.382	4.451	0.412	0.242	0.774
10th percentile	3.859	3.863	4.661	0.682	0.539	0.877
25th percentile	4.685	4.649	5.109	1.002	0.897	1.049
75th percentile	5.975	5.921	6.148	1.672	1.597	1.648
90th percentile	6.419	6.326	6.544	1.941	1.878	1.923
95th percentile	6.659	6.536	6.774	2.101	2.025	2.070
Std deviation	0.995	0.974	0.722	0.524	0.541	0.416
Variance	0.991	0.949	0.521	0.274	0.292	0.173
Max value	7.504	7.550	8.288	2.835	2.786	3.152
Min value	1.268	1.358	3.424	–0.925	–1.103	0.177
Fraction OK	0.715	0.514	0.638	0.715	0.514	0.638

Table 4-14. Summary statistics for travel-time and path-length in the tunnel EDZ for the deposition hole spalling, degraded tunnel EDZ variant case of the amalgamated repository-scale and regional-scale DFN models. For release time 2020 AD, three paths Q1, Q2, and Q3 were tracked for each of 7,483 release locations in the amalgamated model.

	$Log_{10}(t_{EDZ})$ [y]			$Log_{10}(L_{EDZ})$ [m]		
	Q1	Q2	Q3	Q1	Q2	Q3
Mean	–1.447	–1.597	–1.448	1.664	1.539	1.702
Median	–1.430	–1.563	–1.437	1.747	1.647	1.795
5th percentile	–2.772	–3.181	–2.930	0.686	0.178	0.708
10th percentile	–2.417	–2.683	–2.451	0.918	0.727	0.936
25th percentile	–1.933	–2.083	–1.954	1.357	1.192	1.421
75th percentile	–0.932	–1.077	–0.959	2.062	1.996	2.081
90th percentile	–0.421	–0.588	–0.383	2.281	2.231	2.284
95th percentile	–0.161	–0.232	0.006	2.390	2.360	2.401
Std deviation	0.811	0.907	0.882	0.538	0.617	0.537
Variance	0.658	0.822	0.778	0.290	0.381	0.288
Max value	1.336	2.319	2.301	2.981	2.693	3.545
Min value	–5.014	–5.160	–4.794	–0.695	–1.352	–1.034
Fraction OK	0.568	0.581	0.412	0.568	0.581	0.412

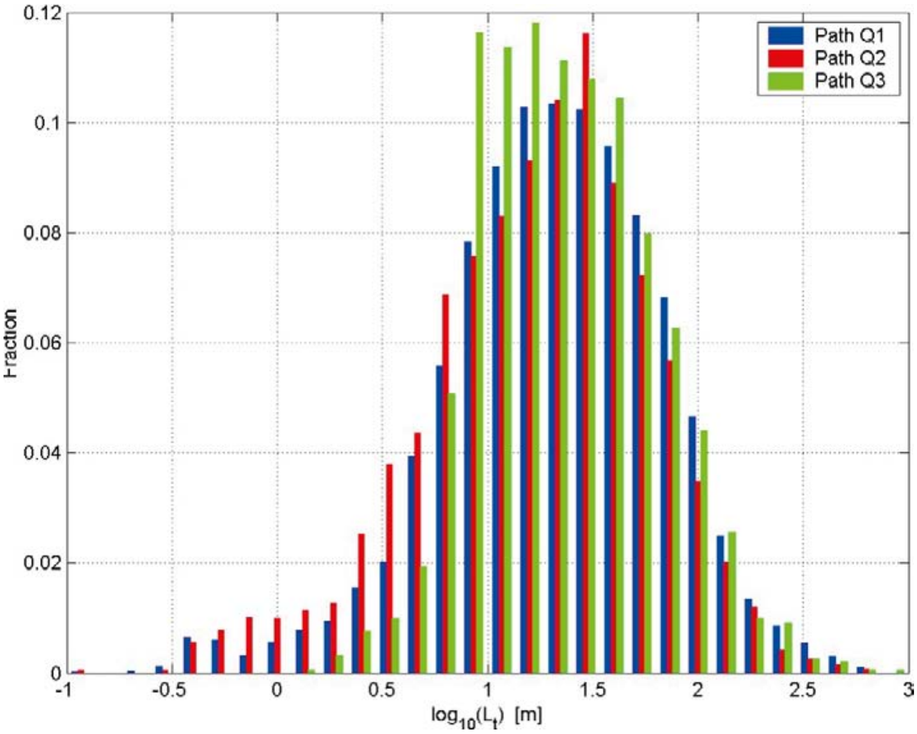

Figure 4-13. *Histograms of path-length in the tunnel, L_t, for paths Q1, Q2 and Q3 in the deposition hole spalling, degraded tunnel EDZ variant of the amalgamated repository-scale and regional-scale DFN models with 7,483 particles released at time 2020 AD.*

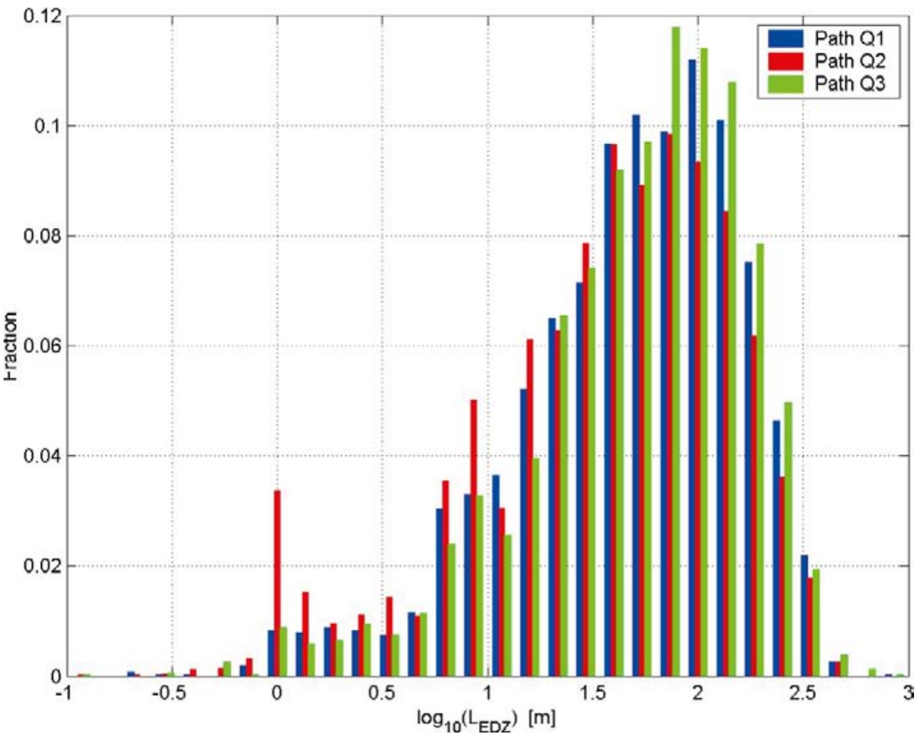

Figure 4-14. *Histograms of path-length in the tunnel EDZ, L_{EDZ}, for paths Q1, Q2 and Q3 in the deposition hole spalling, degraded tunnel EDZ variant of the amalgamated repository-scale and regional-scale DFN models with 7,483 particles released at time 2020 AD.*

5 Summary

Table 5-1 to Table 5-3 show the performance measures for each of the cases considered for the Q1, Q2 and Q3 release points respectively.

It was found that variation of backfill properties in the tunnels had an effect mainly on the tunnel performance measures and indicated that there would be greater flow in the tunnels when the backfill was degraded. However, changing the backfill properties in the central area, ramps and shafts only had minor effects on performance measures for those property values chosen.

The presence of a crown space in the deposition tunnels had a significant effect on the tunnel performance measures and a lesser effect on the rock and tunnel EDZ performance measures. The effect on tunnel performance measures may have been even greater if a crown space had also been modelled in the main and transport tunnels. The effect of degraded tunnel backfill when a crown space was present had an effect on mean travel times and path lengths in the tunnels. The less transmissive tunnel EDZ also had an effect on the tunnel and tunnel EDZ mean travel times and path lengths in the presence of a crown space.

The effect of the deposition hole EDZ and spalling was to increase the travel times and path lengths in the tunnels. Where there was also a degraded deposition tunnel EDZ, there were faster and longer paths in the deposition tunnel EDZ and a reduction in the flow-related transport resistance in the rock. The increased availability of flowing fractures provided by the deposition hole EDZ and spalling increased the number of successful paths for the Q1 release points and provided additional flow pathways around the deposition holes and tunnel EDZ. For the Q2 release points, particles in the degraded EDZ case could be more readily transported to major flowing features, such as deformation zones, leading to the reduction in flow-related transport resistance.

Table 5-1. Mean performance measures in the rock, tunnels and tunnel EDZ for the variant cases of the amalgamated repository-scale and regional-scale DFN models at release time 2020 AD for the Q1 release locations.

Case	t_r [y]	U_r [m/y]	L_r [m]	F_r [y/m]	t_t [y]	L_t [m]	t_{EDZ} [y]	L_{EDZ} [m]
Base	59	$2.2\ 10^{-4}$	1,538	$4.3\ 10^{5}$	$1.2\ 10^{5}$	15	0.49	18
Degraded backfill	47	$2.9\ 10^{-4}$	1,500	$2.6\ 10^{5}$	$4.1\ 10^{4}$	21	0.37	15
Enhanced central area, ramps and shafts	59	$2.2\ 10^{-4}$	1,524	$4.4\ 10^{5}$	$1.2\ 10^{5}$	14	0.50	18
Crown space	51	$2.4\ 10^{-4}$	1,489	$3.0\ 10^{5}$	$4.7\ 10^{4}$	48	0.12	36
Crown space, degraded backfill	49	$2.5\ 10^{-4}$	1,483	$2.9\ 10^{5}$	$2.7\ 10^{4}$	52	0.02	50
Crown space, less transmissive tunnel EDZ	58	$1.7\ 10^{-4}$	1,483	$3.9\ 10^{5}$	$4.7\ 10^{4}$	38	0.15	11
Deposition hole EDZ	49	$2.6\ 10^{-4}$	1,570	$4.8\ 10^{5}$	$1.7\ 10^{5}$	17	0.42	17
Deposition hole EDZ and spalling	404	$1.0\ 10^{-3}$	1,581	$3.4\ 10^{5}$	$2.2\ 10^{5}$	25	0.35	15
Deposition hole EDZ and spalling, degraded deposition tunnel EDZ	262	$2.0\ 10^{-3}$	1,472	$1.7\ 10^{5}$	$1.8\ 10^{5}$	21	0.04	46

Table 5-2. Mean performance measures in the rock, tunnels and tunnel EDZ for the variant cases of the amalgamated repository-scale and regional-scale DFN models at release time 2020 AD for the Q2 release locations.

Case	t_r [y]	U_{EDZ} [m/y]	L_r [m]	F_r [y/m]	t_t [y]	L_t [m]	t_{EDZ} [y]	L_{EDZ} [m]
Base	52	$3.6\ 10^{-4}$	1,618	$2.9\ 10^{5}$	$7.9\ 10^{4}$	13	0.64	23
Degraded backfill	40	$4.0\ 10^{-4}$	1,538	$1.6\ 10^{5}$	$5.9\ 10^{4}$	22	0.51	21
Enhanced central area, ramps and shafts	52	$3.6\ 10^{-4}$	1,589	$3.0\ 10^{5}$	$7.9\ 10^{4}$	12	0.65	22
Crown space	41	$2.7\ 10^{-4}$	1,531	$1.6\ 10^{5}$	$1.0\ 10^{4}$	43	0.15	38
Crown space, degraded backfill	39	$1.6\ 10^{-4}$	1,517	$1.4\ 10^{5}$	$2.7\ 10^{3}$	38	0.13	39
Crown space, less transmissive tunnel EDZ	47	$7.5\ 10^{-6}$	1,503	$2.5\ 10^{5}$	$1.1\ 10^{4}$	31	2.38	21
Deposition hole EDZ	43	$6.4\ 10^{-4}$	1,422	$2.9\ 10^{5}$	$1.2\ 10^{5}$	13	0.28	14
Deposition hole EDZ and spalling	194	$6.7\ 10^{-4}$	1,472	$2.9\ 10^{5}$	$1.9\ 10^{5}$	20	0.27	15
Deposition hole EDZ and spalling, degraded deposition tunnel EDZ	78	$1.5\ 10^{-2}$	1,330	$9.1\ 10^{4}$	$1.7\ 10^{5}$	17	0.03	35

Table 5-3. Mean performance measures in the rock, tunnels and tunnel EDZ for the variant cases of the amalgamated repository-scale and regional-scale DFN models at release time 2020 AD for the Q3 release locations.

Case	t_r [y]	U_t [m/y]	L_r [m]	F_r [y/m]	t_t [y]	L_t [m]	t_{EDZ} [y]	L_{EDZ} [m]
Base	55	$1.0\ 10^{-4}$	1,626	$3.8\ 10^{5}$	$2.7\ 10^{5}$	19	0.71	34
Degraded backfill	38	$3.5\ 10^{-4}$	1,510	$2.6\ 10^{5}$	$2.2\ 10^{4}$	30	0.26	21
Enhanced central area, ramps and shafts	54	$1.0\ 10^{-4}$	1,589	$3.7\ 10^{5}$	$2.7\ 10^{5}$	18	0.73	33
Crown space	41	$1.9\ 10^{-4}$	1,486	$1.6\ 10^{5}$	$2.7\ 10^{5}$	53	0.10	24
Crown space, degraded backfill	38	$2.1\ 10^{-4}$	1,514	$1.3\ 10^{5}$	$3.2\ 10^{4}$	47	0.04	50
Crown space, less transmissive tunnel EDZ	48	$5.5\ 10^{-5}$	1,500	$2.2\ 10^{5}$	$1.9\ 10^{5}$	41	1.43	19
Deposition hole EDZ	48	$1.0\ 10^{-4}$	1,452	$3.8\ 10^{5}$	$3.9\ 10^{5}$	20	0.45	18
Deposition hole EDZ and spalling	179	$1.6\ 10^{-4}$	1,493	$3.5\ 10^{5}$	$4.6\ 10^{5}$	26	0.37	15
Deposition hole EDZ and spalling, degraded deposition tunnel EDZ	93	$5.2\ 10^{-4}$	1,371	$1.5\ 10^{5}$	$4.3\ 10^{5}$	23	0.04	50

References

SKB's (Svensk Kärnbränslehantering AB) publications can be found at www.skb.se/publications.

Hartley L, Hoch A, Jackson P, Joyce S, McCarthy R, Swift B, Gylling B, Marsic N, 2006. Groundwater flow and transport modelling during the temperate period for the SR-Can assessment. Laxemar subarea – version 1.2. SKB R-06-99, Svensk Kärnbränslehantering AB.